

Contract NAS8-20399

A STUDY OF INTERNAL MAGNETIC FIELDS FOR HIGH ENERGY
FORMING AND STRUCTURAL ASSEMBLY

REPORT

FOR THE PERIOD


APRIL 1, 1966 THRU JUNE 30, 1967

By

D. D. Wier, B. J. Ball
L. J. Hill, and G. S. Hyde

June 26, 1967

PRINCIPAL INVESTIGATOR:


D. D. Wier
Associate Professor
Department of Electrical Engineering
Mississippi State University
Drawer EE, State College, Mississippi 39762
Telephone: 601+323-4321, Ext. 396

Contract NAS8-20399

A STUDY OF INTERNAL MAGNETIC FIELDS FOR HIGH ENERGY
FORMING AND STRUCTURAL ASSEMBLY

By

D. D. Wier, B. J. Ball
L. J. Hill, and G. S. Hyde

Department of Electrical Engineering
Mississippi State University
State College, Mississippi

ABSTRACT

A beryllium coil assembly, referred to as the hammer coil, was developed by the George C. Marshall Space Flight Center in Huntsville, Alabama. This coil is being used to smooth and shape metallic materials with the advantage of reducing work hardening and fatigue.

This study was made to determine the maximum static force at points on different materials being subjected to an intense magnetic field produced by the hammer coil.

The forces were found to be independent of the thickness of the material if the thickness is greater than the depth of current penetration. The values of force were found to vary inversely to the values of the resistivity of the material.

TABLE OF CONTENTS

Chapter	Page
LIST OF TABLES	iv
LIST OF FIGURES	vi
SUMMARY	1
I. INTRODUCTION	2
II. METHOD OF APPROACH	5
A. General Description of Coil and Plate	5
B. Force on Current-Carrying Conductor in Magnetic Field	5
C. Procedure to Determine Forces	10
III. APPLICATION OF METHOD	13
A. Determination of Resistance	13
B. Determination of Induced Voltage	14
C. Determination of Current	21
D. Determination of Force	21
IV. Analysis of Results	24
V. CONCLUSION	38
APPENDIX A	40
APPENDIX B	42
APPENDIX C	56
REFERENCES	58
BIBLIOGRAPHY	59

LIST OF TABLES

Table	Title	Page
1.	The Characteristics of Aluminum Alloys	4
2.	The Resistivity and the Corresponding Penetration Depth for Each Material Studied	4
3.	The Distance Z from the Surface of the Coil to a Point of Average Current in the Segments of a Plate for the Thicknesses of (a) 0.9525, 1.2700, and 1.9050 Centimeters and (b) 0.1524 Centimeters	19
4.	The Magnetic Field Intensity and the Resultant Angles Obtained from the Curves in Appendix B with Z Equal 0.2959 Centimeters	19
5.	The Theoretical Values of Force, Pressure, and Resultant Angle as a Function of the Radial Distance y on Sheets of Materials with a Resistivity of 5.9 Microhm-Centimeters and Thicknesses of 0.9525, 1.2700, and 1.9050 Centimeters.	27
6.	The Theoretical Values of Force, Pressure, and Resultant Angle as a Function of the Radial Distance y on Sheets of Materials with a Resistivity of 5.4 Microhm-Centimeters and Thicknesses of 0.9525, 1.2700, and 1.9050 Centimeters.	28
7.	The Theoretical Values of Force, Pressure, and Resultant Angle as a Function of the Radial Distance y on Sheets of Materials with a Resistivity of 5.2 Microhm-Centimeters and Thicknesses of 0.9525, 1.2700, and 1.9050 Centimeters	29
8.	The Theoretical Values of Force, Pressure, and Resultant Angle as a Function of the Radial Distance y on Sheets of Materials with a Resistivity of 4.0 Microhm-Centimeters and Thicknesses of 0.9525, 1.2700, and 1.9050 Centimeters	30
9.	The Theoretical Values of Force, Pressure, and Resultant Angle as a Function of the Radial Distance y on Sheets of Materials with a Resistivity of 5.9 Microhm-Centimeters and a Thickness of 0.1524 Centimeters.....	31

LIST OF TABLES--Continued

Table	Title	Page
10.	The Theoretical Values of Force, Pressure, and Resultant Angle as a Function of the Radial Distance y on Sheets of Materials with a Resistivity of 5.4 Microhm-Centimeters and a Thickness of 0.1524 Centimeters	32
11.	The Theoretical Values of Force, Pressure, and Resultant Angle as a Function of the Radial Distance y on Sheets of Materials with a Resistivity of 5.2 Microhm-Centimeters and a Thickness of 0.1524 Centimeters	33
12.	The Theoretical Values of Force, Pressure, and Resultant Angle as a Function of the Radial Distance y on Sheets of Materials with a Resistivity of 4.0 Microhm-Centimeters and a Thickness of 0.1524 Centimeters	34

LIST OF FIGURES

Figure	Title	Page
1-a.	A Picture of the High Energy Capacitor Unit and the Hammer Coil	6
1-b.	A Picture of the Hammer Coil	7
2.	A Simplified Schematic Circuit Diagram of the Hammer Coil and the Power Supply	8
3.	An Edge View of the Hammer Coil and a Sheet of Material at the Instant of Initial Charge	9
4.	A Sketch of the Hammer Coil's Current Wave Indicating an Approximate Natural Frequency of 3,300 Hz	12
5.	The Representation of One Coil-Turn and One Plate Segment for Determining Z	16
6.	The Waveform of an Induced Voltage in an Actual Circular Segment as a Function of Time	35
7.	A Plot of the Experimental Data of an Induced Voltage V in the Actual Circular Segments as a Function of the Radial Distance y	36
8.	A Plot of the Theoretical Values of an Induced Voltage per Coil Ampere as a Function of the Radial Distance y	37
B-1.	A Plot of the Magnetic Field Intensity and the Resultant Angle as a Function of the Distance Normal to the Surface of the Hammer Coil for a Constant Radial Value, y, of 0.5207 Centimeters	42
B-2.	A Plot of the Magnetic Field Intensity and the Resultant Angle as a Function of the Distance Normal to the Surface of the Hammer Coil for a Constant Radial Value, y, of 1.0663 Centimeters	43
B-3.	A Plot of the Magnetic Field Intensity and the Resultant Angle as a Function of the Distance Normal to the Surface of the Hammer Coil for a Constant Radial Value, y, of 1.6119 Centimeters	44

LIST OF FIGURES--Continued

Figure	Title	Page
B-4.	A Plot of the Magnetic Field Intensity and the Resultant Angle as a Function of the Distance Normal to the Surface of the Hammer Coil for a Constant Radial Value, y, of 2.1575 Centimeters	45
B-5.	A Plot of the Magnetic Field Intensity and the Resultant Angle as a Function of the Distance Normal to the Surface of the Hammer Coil for a Constant Radial Value, y, of 2.7031 Centimeters	46
B-6.	A Plot of the Magnetic Field Intensity and the Resultant Angle as a Function of the Distance Normal to the Surface of the Hammer Coil for a Constant Radial Value, y, of 3.2487 Centimeters	47
B-7.	A Plot of the Magnetic Field Intensity and the Resultant Angle as a Function of the Distance Normal to the Surface of the Hammer Coil for a Constant Radial Value, y, of 3.7943 Centimeters	48
B-8.	A Plot of the Magnetic Field Intensity and the Resultant Angle as a Function of the Distance Normal to the Surface of the Hammer Coil for a Constant Radial Value, y, of 4.3398 Centimeters	49
B-9.	A Plot of the Magnetic Field Intensity and the Resultant Angle as a Function of the Distance Normal to the Surface of the Hammer Coil for a Constant Radial Value, y, of 4.8854 Centimeters	50
B-10.	A Plot of the Magnetic Field Intensity and the Resultant Angle as a Function of the Distance Normal to the Surface of the Hammer Coil for a Constant Radial Value, y, of 5.4310 Centimeters	51
B-11.	A Plot of the Magnetic Field Intensity and the Resultant Angle as a Function of the Distance Normal to the Surface of the Hammer Coil for a Constant Radial Value, y, of 5.9766 Centimeters	52

LIST OF FIGURES--Continued

Figure	Title	Page
B-12.	A Plot of the Magnetic Field Intensity and the Resultant Angle as a Function of the Distance Normal to the Surface of the Hammer Coil for a Constant Radial Value, y, of 6.5222 Centimeters	53
B-13.	A Plot of the Magnetic Field Intensity and the Resultant Angle as a Function of the Distance Normal to the Surface of the Hammer Coil for a Constant Radial Value, y, of 7.0678 Centimeters	54
B-14.	A Plot of the Magnetic Field Intensity and the Resultant Angle as a Function of the Distance Normal to the Surface of the Hammer Coil for a Constant Radial Value, y, of 7.6134 Centimeters	55

A STUDY OF INTERNAL MAGNETIC FIELDS FOR HIGH ENERGY
FORMING AND STRUCTURAL ASSEMBLY

SUMMARY

A beryllium coil assembly, referred to as the hammer coil, was developed by the George C. Marshall Space Flight Center in Huntsville, Alabama. This coil is being used to smooth and shape metallic materials with the advantage of reducing work hardening and fatigue.

This study was made to determine the maximum static force at points on different materials being subjected to an intense magnetic field produced by the hammer coil.

The induced voltage was determined in assumed concentric circular segments of the sheet of material using Faraday's law. The current could then be determined by dividing by the resistance of each segment. Therefore, using a form of Lorentz's force equation the maximum force on each segment was calculated.

The forces were found to be independent of the thickness of the material if the thickness is greater than the depth of current penetration. This depth was defined as the point where the current has a value of $1/3e$ times the value at the surface. The largest static force occurred at points 4.6127 centimeters radially out from the center line of the hammer coil. The values of force were found to vary inversely to the values of the resistivity of the material. The diameter of this hammer coil is 10.3175 centimeters.

CHAPTER I

INTRODUCTION

The purpose of this study is to determine the maximum force on a static sheet of metallic material subjected to a magnetic field produced by a beryllium coil assembly. This coil, referred to as the hammer coil, is now being used at the George C. Marshall Space Flight Center in Huntsville, Alabama.

The hammer coil is used to smooth and shape metal material with the advantage of reducing work hardening and fatigue. This shaping and smoothing process is accomplished by an intense magnetic field generated by the hammer coil. The time-varying magnetic field induces a voltage in the metal creating a magnetic field in opposition to the one generated by the coil. These opposing magnetic fields create a force between the coil and sheet of material.

This study is directly concerned with the maximum forces produced on four thicknesses of six different alloys. The thicknesses under consideration are 0.1524, 0.9525, 1.2700, and 1.9050 centimeters. These alloys and some of their characteristics are listed in Table 1. The values of electrical and magnetic properties were furnished through the courtesy of the Aluminum Company of America.

This is the second stage of a series of studies being made on the hammer coil which is being conducted on a contract basis through the Department of Electrical Engineering at Mississippi State University. The purpose of the initial study was to determine the impedance characteristics of the coil. The computer program given in Appendix A is a result of this initial study.¹ It is designed to give the vector

magnetic potential and magnetic field intensity at various points out from the face of the coil. This data will be used to determine the flux linking imaginary segments in the sheet of material subjected to the intense magnetic field produced by the coil. From this flux linkage the induced emf in the segment may be determined and the resulting current in the segment may be found. The force acting upon a current-carrying conductor in a magnetic field where the conductor is perpendicular to the magnetic lines is given by

$$F = BLI, \quad (1)$$

where B is the magnetic flux density, L is the length of the conductor, and I is the current in the conductor.²

Alloy	Temper	Relative Magnetic Permeability	Conductivity @ 20C	Resistivity @ 20C
			% International Annealed-Cooper Standard	(Microhm-Centimeter)
2219	T87	1.0000196	32	5.4
7075	T6	1.0000159	33	5.2
7075	T651	1.0000159	33	5.2
6061	T6	1.0000199	43	4.0
5456	H343	1.0000200 *	29	5.9
5456	H321	1.0000200 *	29	5.9

*Estimated Value

Table 1. The Characteristics of Aluminum Alloys.

Resistivity ρ (ohm-meters)	Penetration Depth δ (cm)
5.9×10^{-8}	0.2131
5.4×10^{-8}	0.2037
5.2×10^{-8}	0.1999
4.0×10^{-8}	0.1755

Table 2. The Resistivity and the Corresponding Penetration Depth for Each Material Studied.

CHAPTER II

METHOD OF APPROACH

A. GENERAL DESCRIPTION OF COIL AND PLATE

Shown in Figures 1-a and 1-b are pictures of the high energy capacitor discharge power supply and the hammer coil, respectively. An equivalent circuit of this power supply and coil was determined in the initial study as shown in Figure 2. Given in Figure 3 is an edge view representation of the hammer coil resting on a sheet of material at the instant of the initial charge. This is the position where the maximum static force must be calculated at points radially out from the center line of the coil. As shown in this figure the plate is assumed to consist of 14 concentric circular segments with a width of 0.5456 centimeters. This number was chosen since, as will be seen later, the force is negligible beyond this point.

B. FORCE ON CURRENT-CARRYING CONDUCTOR IN MAGNETIC FIELD

The following equation,

$$\vec{F} = q\vec{v} \times \vec{B}, \quad (2)$$

is known as Lorentz's force equation.³ \vec{F} is the force on a moving charge q with a velocity \vec{v} in a magnetic field of flux density \vec{B} . This equation may be expressed as

$$F = BLI \sin \theta \quad (3)$$

for a conductor of length L carrying a current I in a magnetic field B . The angle θ is the angle that the conductor makes with the direction of the magnetic field and in this study will be 90 degrees. So, Equation (3) becomes

$$F = BLI \quad (4)$$

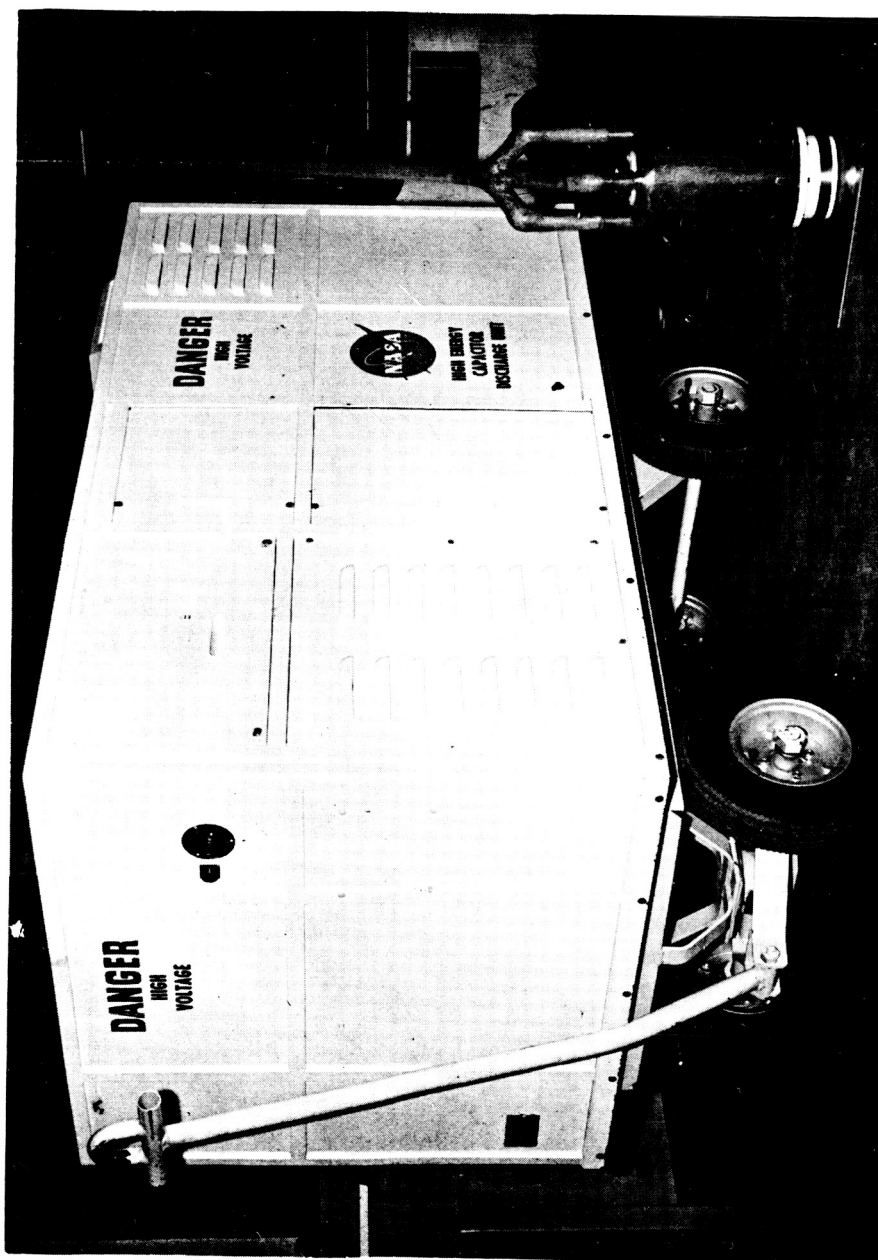


Figure 1-a. A Picture of the High Energy Capacitor Discharge Unit and the Hammer Coil.

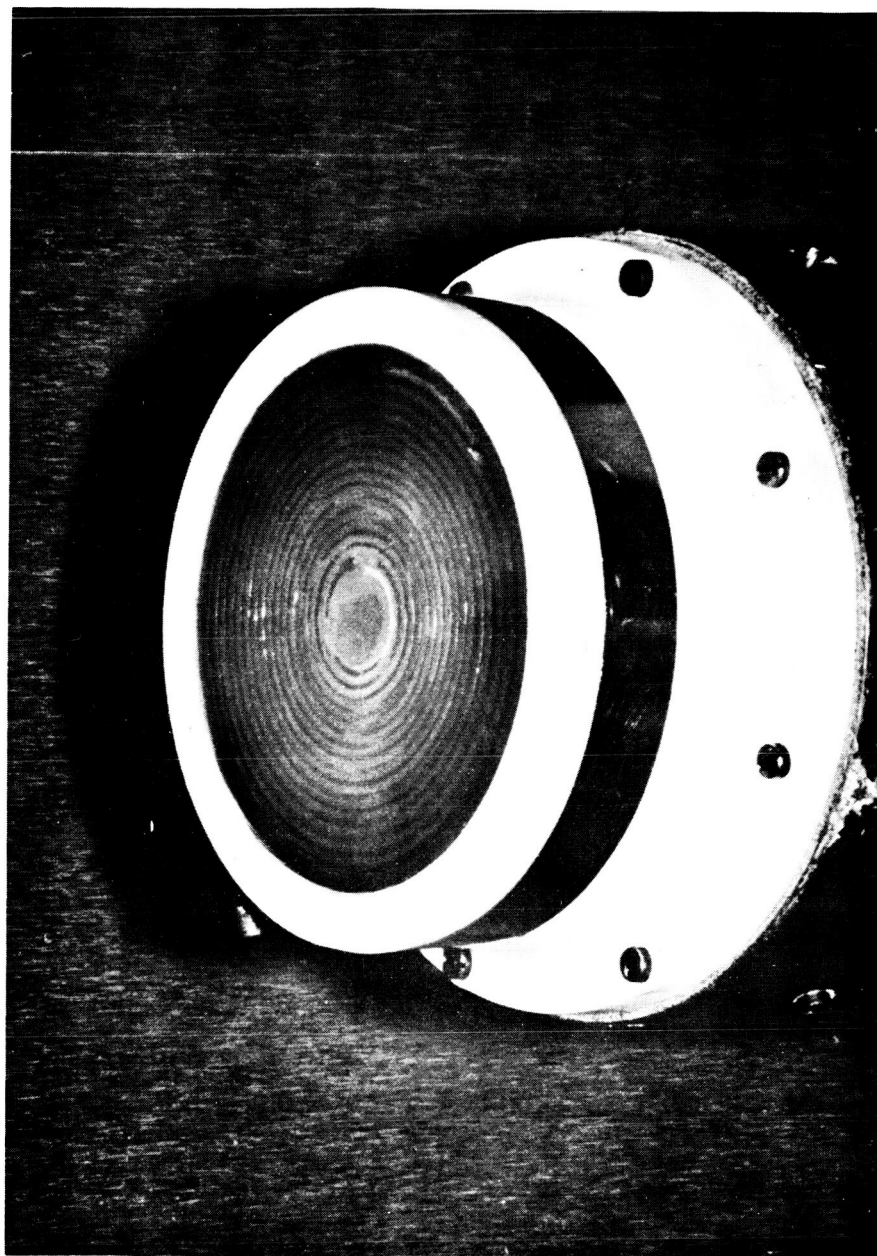


Figure 1-b. A Picture of the Hammer Coil.

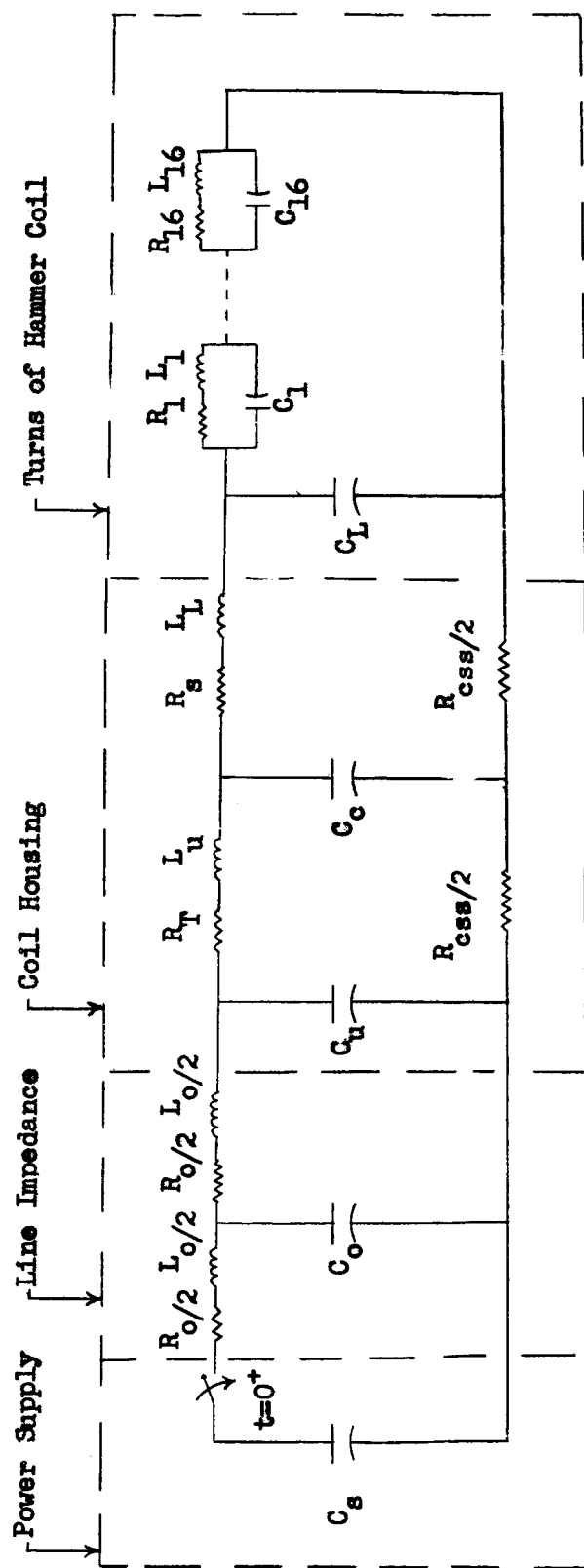


Figure 2. A Simplified Schematic Circuit Diagram of the Hammer Coil and the Power Supply.

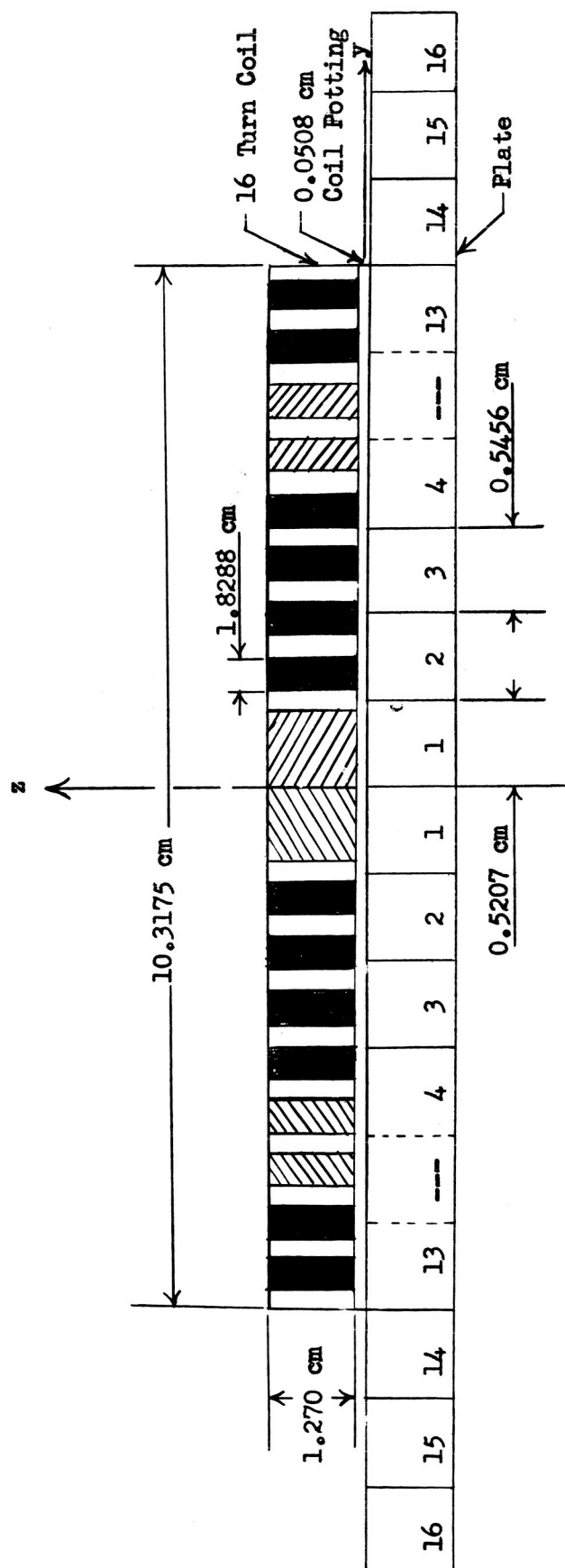


Figure 3. An Edge View of the Hammer Coil and a Sheet of Material at the Instant of Initial Charge.

where F is in newtons, B is in webers per square meter, L is in meters, and I is in amperes.

C. PROCEDURE TO DETERMINE FORCES

As explained, it is assumed that the sheet of material is made up of concentric circular segments with their center lying on the center line of the hammer coil. Using Equation (4) the force on each assumed segment may be calculated if the current in each segment can be determined. The length of each segment is known by using

$$L_n = 2\pi r_n, \quad (5)$$

where r_n is average radius of segment n. Also, B, the magnetic flux density, is known since the magnetic field intensity was determined in the initial study of the hammer coil.

The current in each segment may be found by dividing the resistance of the segment into the voltage induced in the segment by the magnetic field. The resistance may be found using

$$R_n = \frac{\rho L_n}{A}, \quad (6)$$

where ρ is the resistivity of the material, L_n is the length of the segment, and A is the cross-sectional area of the segment.⁴ The induced voltage may be determined by applying Faraday's law which says that an emf is induced in an electric circuit whenever the magnetic flux linking the circuit changes.⁵ For each segment this law may be expressed

$$e_n(t) = \frac{\Delta \phi_n}{\Delta T}, \quad (7)$$

where $\Delta \phi_n$ is the magnetic flux linking the segment in ΔT time. From a photograph of the current wave of the hammer coil furnished by the Marshall Space Flight Center at Huntsville, Alabama, the approximate

natural frequency is 3,300 Hz. This trace is duplicated in Figure 4. The maximum magnetic flux occurred at 1/4 the period, T, therefore,

$$T = \frac{1}{(4)(3300)} \text{ seconds.} \quad (8)$$

From Figure 3 it may be seen that the only component of the magnetic field intensity, H_R , inducing voltage in the segments is H_z which is normal to the surface of the sheet. The flux, $\Delta\phi_n$, therefore may be determined by calculating the average value of H_z out to the segment and multiplying this average value by the surface area and the permeability of the medium.

The current in each segment may now be determined, and using Equation (4) the maximum static force on each segment or at points radially out from the center line of the coil may be determined.

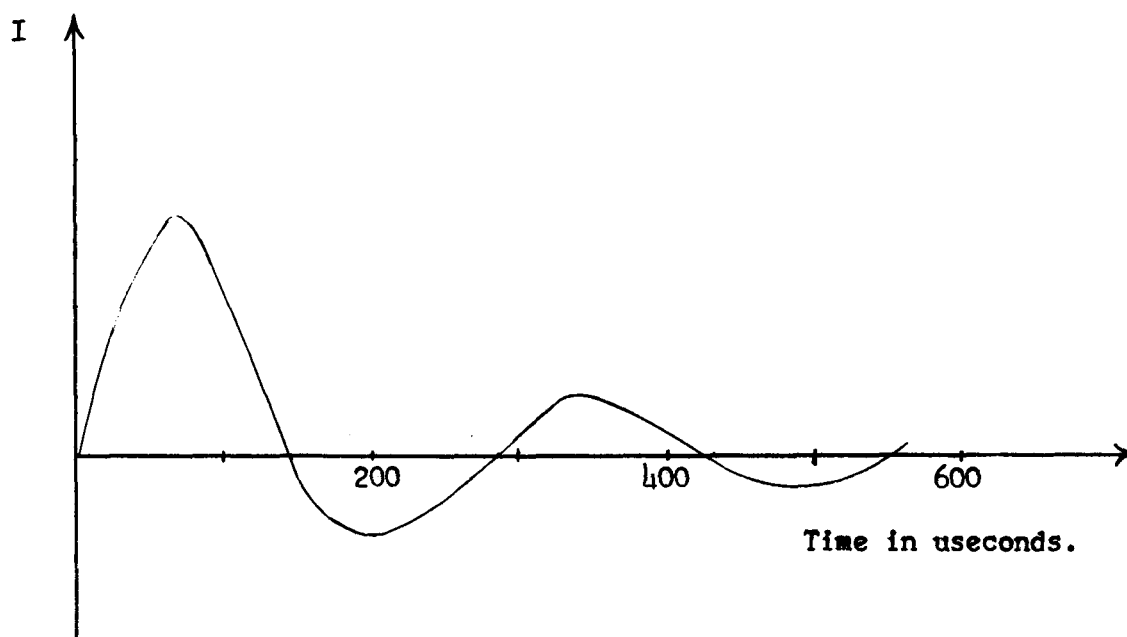


Figure 4. A Sketch of the Hammer Coil's Current Wave Indicating an Approximate Natural Frequency of 3,300 Hz.*

* Furnished by Marshall Space Flight Center in Huntsville, Alabama.

CHAPTER III

APPLICATION OF METHOD

A. DETERMINATION OF RESISTANCE

The resistance of each concentric circular segment must be determined in order to find the current generated in each segment

This resistance may be obtained from the following formula,

$$R = \frac{\rho L}{A} , \quad (9)$$

where R is the resistance in ohms, ρ is the resistivity of the material in ohm-meters, L is the average length of the circular segment in meters, and A is the cross-sectional area of the conducting material in square meters.⁶ From Skilling it is found that the depth of current penetration, δ , is given by

$$\delta = \sqrt{\frac{\rho}{\pi f \mu}} , \quad (10)$$

where δ is the current penetration depth in meters, ρ is the resistivity in ohm-meters, f is the frequency, and μ is the permeability of the medium in henrys per meter.⁷ δ is the depth of penetration at which the induced voltage is 1/e times the value of the induced voltage at the surface.

Therefore, A of Equation (9) is given by

$$A = \delta \cdot h , \quad (11)$$

where h is the width of the circular segment in meters.

From Figure 4 it was determined that the approximate natural frequency is 3,300 Hz. So, from Equation (10) a corresponding value of δ may be calculated for each value of ρ . Using the permeability of free space ($4\pi \times 10^{-7}$ henry per meter) these results are shown in Table 2.

At this point it must be noted that if the penetration depth is greater than the actual thickness of the material the actual thickness should be used to calculate A. In this study all of the thicknesses are greater than the δ values given in Table 2 except the material with the thickness of 0.1524 centimeters. Also, it should be noticed that δ is independent of the thickness of the material, but it is inversely proportional to the square root of the frequency.

The method of calculating the maximum static force on the various assumed segments is illustrated by an example calculation which will be made in each section throughout the rest of this chapter. This example will ultimately determine the force produced on segment 3 shown in Figure 3. The resistivity of the material will equal 5.9×10^{-8} ohm-meters.

From Equations (9) and (11) the resistance of the nth segment may be determined from the following,

$$R_n = \frac{\rho \cdot 2\pi r_n}{\delta \cdot h} \quad (12)$$

where r_n is the average radius of the nth circular segment. Using Equation (12) the resistance of the third segment is calculated as follows,

$$\begin{aligned} R_3 &= \frac{\rho \cdot 2\pi r_3}{\delta \cdot h} \\ &= \frac{(5.9 \times 10^{-8})(2\pi)(1.3391 \times 10^{-2})}{(0.2131 \times 10^{-2})(0.5456 \times 10^{-2})} \\ R_3 &= 42.75 \times 10^{-5} \text{ ohms.} \end{aligned}$$

B. DETERMINATION OF INDUCED VOLTAGE

The voltage induced in each segment may be calculated using

Faraday's law or Equation (7) expressed as⁸

$$e_n(t) = \frac{\Delta\phi_n}{\Delta T} . \quad (13)$$

To use this expression the change in flux during ΔT time must be determined.

Using the computer program in Appendix A the magnetic field intensity and the resultant angle are determined as a function of y radially out from the center line of the hammer coil and as a function of z normal to the surface of the coil.⁹ These directional axes are shown in Figure 3. The magnetic field intensity was calculated by the program on a per coil ampere basis. Given in Appendix B are 14 graphs with H_R and θ_R plotted as a function of z holding y constant. These constant y values were chosen at the points of intersection of the assumed circular segments shown in Figure 3. Using graphs the magnetic field intensity may be determined at any reasonable point out from the surface of the coil or for different values of penetration depth. It should be noted that these plots can only be used when the plate is assumed to consist of concentric circular segments having an inner and outer radius of the constant y values plotted.

The value of z used to read H_R and θ_R from the plots for a certain δ value is determined by

$$Z = M + P , \quad (14)$$

where M is the 0.0508 centimeters separation between the plate and coil due to the potting of the coil and P is the distance from the surface of the plate to the center of the current concentration. Shown in Figure 5 is a representation of this Z value related on one segment of the plate. Since P is the point in the material where the current

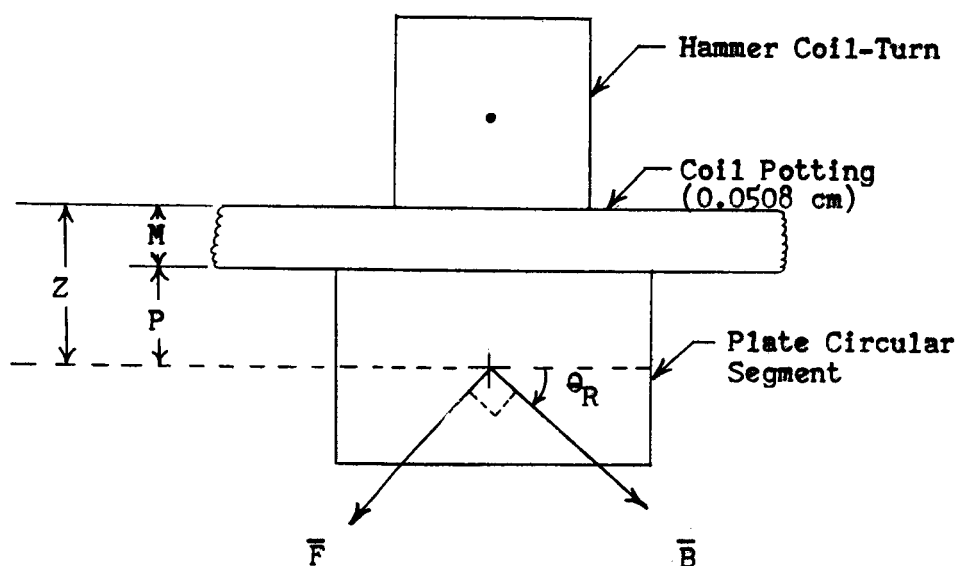


Figure 5. The Representation of One Coil-Turn and One Plate Segment for Determining Z .

is equal to its average value, integration may be used to determine P. The skin effect current equation is given as follows,

$$I = I_M e^{-z/\delta} , \quad (15)$$

where z is the independent variable, δ is the penetration depth, and I_M is the maximum value of the current at the surface of the plate.¹⁰ So, the average current is determined as some proportion of the maximum current as follows,

$$\begin{aligned} I_{av} &= \frac{1}{3\delta} \int_0^{3\delta} I_M e^{-z/\delta} dz \\ &= -\frac{I_M}{3} (e^{-3} - 1) \\ I_{av} &= 0.317 I_M. \end{aligned} \quad (16)$$

Therefore, the value of P is determined from the following,

$$\begin{aligned} 0.317 I_M &= I_M e^{-P/\delta} \\ \ln(0.317) &= -\frac{P}{\delta} \\ P &= 1.15 \delta . \end{aligned} \quad (17)$$

For a material with a thickness less than the penetration depth, the average current is found by integrating over the thickness. In this study the only material with a thickness less than the penetration depth is the 0.1524 centimeter sheet. The formula for the average current is determined as follows,

$$\begin{aligned} I_{av} &= \frac{1}{0.1524} \int_0^{0.1524} I_M e^{-z/\delta} dz \\ I_{av} &= \frac{\delta I_M}{0.1524} (1 - e^{-0.1524/\delta}) . \end{aligned} \quad (18)$$

For a resistivity of 5.9×10^{-8} ohm-meters and a corresponding δ of 0.2131 centimeters the average current may be calculated using Equation (18) as follows,

$$I_{av} = \frac{0.2131}{0.1524} I_M (1 - e^{-\frac{0.1524}{0.2131}})$$

$$I_{av} = 0.713 I_M \quad (19)$$

Therefore, using Equation (15) the value of P is determined as

$$0.713 I_M = I_M e^{-P/0.2131}$$

$$\ln(0.713) = -\frac{P}{0.2131}$$

$$P = 0.07214 \text{ centimeters.}$$

Similarly, the remaining values of δ are used to calculate the values of P for materials with a thickness of 0.1524 centimeters.

The values of Z are given in Table 3 for the corresponding values of δ and material thickness. For thicknesses of 0.9525, 1.2700, and 1.9050 centimeters the values of Z are equal since the penetration depth is independent of the material thickness. However, this is not the case for the material with a thickness of 0.1524 centimeters since δ is greater than the material's thickness.

Since the flux normal to the surface of the material is used to compute the induced voltage, the only component of interest is H_z . If the average value of H_z is found within the circular segment and multiplied by the surface area and the permeability of the medium, the magnetic flux linking the segment is determined. To illustrate this procedure an example will be used. For the resistivity of 5.9×10^{-8} ohm-meters the value of Z given in Table 3 is 0.2959 centimeters.

Resistivity ρ (ohm-meters)	Penetration Depth δ (cm)	$Z = 1.15 \delta + 0.0508$ (cm)
5.9×10^{-8}	0.2131	0.2959
5.4×10^{-8}	0.2037	0.2852
5.2×10^{-8}	0.1999	0.2809
4.0×10^{-8}	0.1755	0.2530

(a)

Resistivity ρ (ohm-meters)	Penetration Depth δ (cm)	$Z = \delta + 0.0508$ (cm)
5.9×10^{-8}	0.1524	0.2008
5.4×10^{-8}	0.1524	0.2007
5.2×10^{-8}	0.1524	0.2006
4.0×10^{-8}	0.1524	0.2004

(b)

Table 3. The Distance Z from the Surface of the Coil to a Point of Average Current in the Segments of a Plate for the Thicknesses of (a) 0.9525, 1.2700, and 1.9050 Centimeters and (b) 0.1524 Centimeters.

y (cm)	H_R (amperes/meter-coil ampere)	θ_R (degrees)
* 0.0000	.00	90.00
0.5207	113.25	78.80
1.0663	122.75	63.57
1.6119	127.90	42.23

* Assumed Values at $y = 0$

Table 4. The Magnetic Field Intensity and the Resultant Angles Obtained from the Curves in Appendix B with Z Equal 0.2959 Centimeters.

Using this value of Z , the data shown in Table 4 was obtained from the curves in Appendix B. The H_z component may be calculated from this data using the following relationship,

$$H_z = H_R \sin \theta_R . \quad (20)$$

The average value of H_z out to the third segment may be determined by using Simpson's rule given as follows,

$$A = \frac{H}{3} \cdot \left[H_{z_1} + 4H_{z_2} + H_{z_3} \right] \quad (21)$$

Where A is the area under the curve between H_{z_1} and H_{z_3} and H is the width of the circular segment.¹¹ Equation (21) is divided by the inner radius of the segment to obtain the average value of H_z as follows,

$$H_{za} = \frac{H}{3r_i} \cdot \left[H_{z_1} + 4H_{z_2} + H_{z_3} \right] , \quad (22)$$

where r_i is the inner radius of the segment. Using the data in Table 4 and Equations (20) and (22), H_{za} is calculated as follows for our example.

$$H_{za} = \frac{(0.5456)}{3(1.0663)} \cdot \left[0 + 4(111.10) + 109.97 \right]$$

$$H_{za} = 94.80 \text{ amperes/meter-coil ampere.}$$

The average value of H_z is now multiplied by the permeability and surface area to obtain the magnetic flux linking the third segment given as follows,¹²

$$\phi = H_{za} \cdot \mu_0 \cdot \pi r_i^2 \quad (23)$$

$$= (94.80)(4\pi \times 10^{-7})(\pi)(1.0663 \times 10^{-2})^2$$

$$\phi = 4.25 \times 10^{-8} \text{ webers/coil ampere.}$$

The value of ΔT determined by Equation (8) is $1/(4)(3300)$ seconds. Therefore, using Equation (13) the voltage induced in the third segment is

$$\begin{aligned} e_3 &= \frac{\Delta\phi}{\Delta T} \\ &= \frac{4.25 \times 10^{-8}}{1/(4)(3300)} \\ e_3 &= 5.615 \times 10^{-4} \text{ volts/coil ampere.} \end{aligned}$$

C. DETERMINATION OF CURRENT

The current in each segment of the plate may be found by dividing the induced voltage by the resistance of the segment. Since the magnetic field intensity was determined on a per ampere basis, the current in each segment is also a function of the coil current.¹³

In the example the values of resistance and voltage have already been determined. Therefore, the current in the third segment is given as,

$$\begin{aligned} I_3 &= \frac{e_3}{R_3} \\ &= \frac{5.615 \times 10^{-4}}{42.75 \times 10^{-5}} \\ I_3 &= 1.313 \text{ amperes/coil ampere.} \end{aligned}$$

D. DETERMINATION OF FORCE

Since the magnetic field intensity is perpendicular to the current carrying segments shown in Figure 3, the force on each segment may be expressed as¹⁴

$$F = B_R LI \quad . \quad (24)$$

In our study B_R is the resultant magnetic flux density per coil ampere

at the point of average current in the segment, L is the average length of segment in meters, and I is the current in the segment per ampere of coil current. From Equation (24) the force on each segment will be determined in pounds per coil ampere squared in the direction of some angle θ_F . The angle θ_F is determined from the following,

$$\theta_F = - \left[\theta_R + 90^\circ \right] , \quad (25)$$

where θ_R is the resultant angle of the magnetic field intensity.

Equation (25) gives the direction of the force in the direction of $\bar{L} \times \bar{B}_R$ which is perpendicular to the plane made by \bar{L} and \bar{B} . This perpendicular direction is determined by the direction of advance of a right-handed screw as \bar{L} is turned into \bar{B}_R .¹⁵ Figure 5 indicates the direction of the force with the segment current going into the plane of the paper. The clock-wise direction from the reference line in Figure 5 will be assumed to yield a negative angle. Since θ_R was determined assuming the coil's face was up instead of down, the negative value of θ_R must be used as given in Equation (25).

In our example the value of B_R is determined from the graphs in Appendix B. The values of H_R and θ_R for Z equal 0.2959 centimeters for three consecutive values of y including the inner and outer radius of the third segment are given in Table 4. By assuming a parabolic curve, the value of H_R at the center of segment three may be determined from the following equation:

$$H_R = B_0 + B_1 y + B_2 y^2 , \quad (26)$$

where B_0 , B_1 , and B_2 are calculated constants. These constants are solved from three independent equations in the form of Equation (26) using the values of H_R and y given in Table 4. The same method is

used to determine the value of θ_R at the center of the segment. Using the digital computer, as will be discussed later for solving the complete process, the values of H_R and θ_R were calculated as 124.50 amperes/meter-coil ampere and 51.98 degrees, respectively.

The force on the third segment may now be determined as follows,

$$\begin{aligned} F_3 &= B_R L I \sin \theta_R \\ &= (4\pi \times 10^{-7})(124.50)(2\pi)(1.3391 \times 10^{-2})(1.312) \sin(-51.98^\circ - 90^\circ) \\ &= 0.1731 \times 10^{-4} \sin(-141.98^\circ) \text{ newtons/coil ampere}^2*. \end{aligned} \quad (27)$$

The pressure on each segment may be determined from the following formula,

$$P = \frac{F}{2\pi r H}, \quad (28)$$

where P is the pressure in newtons per square meter-coil ampere, r is the average radius of the segment in meters, and H is the width of the segment in meters. Therefore, for segment three in our example the pressure is calculated as follows,

$$\begin{aligned} P_3 &= \frac{F_3}{2\pi r H} \\ P_3 &= \frac{0.1731 \times 10^{-4} \sin(-141.98^\circ)}{(2\pi)(1.3391 \times 10^{-2})(0.5456 \times 10^{-2})} \\ P_3 &= 3.76 \times 10^{-2} \text{ newtons/meter}^2\text{-coil ampere}^2. \end{aligned}$$

*Convert newtons to pounds by multiplying by 0.225 pounds/newtons.

CHAPTER IV

ANALYSIS OF RESULTS

Throughout Chapter III an example was used to illustrate each step in the calculation of the static forces. This was done for only one segment of a material with a certain resistivity and thickness. Therefore, because of the long laborious process of calculating these forces for several materials with 14 assumed segments, use must be made of the digital computer. Given in Appendix C is a program designed to determine the force and pressure in the center of each segment of the plate shown in Figure 3. The information required to run this program is the resistivity of the material, penetration depth, Z from Equation (14), and the values of H_R and θ_R from the graphs in Appendix B. Given in Table 3 are eight different combinations of resistivity and thickness for which the forces and pressures are calculated. Using the IBM 360 computer the results are given in Tables 5 through 12. From these results it is determined that the maximum force occurred at points 4.6127 centimeters radially out from the center line of the hammer coil. Also, the values of force varied inversely to the values of resistivity. This was true for both the materials with a thickness greater than the penetration depth and less than the penetration depth.

Because of the complexity of obtaining exact experimental results due to a large number of variables, it was thought best to verify the theoretical method of this study by comparing three main results. First, the natural frequency of the induced voltage in the circular segments is approximately 3,300 Hz. Second, the experimental values of the induced

voltage in the segments have the same waveshape as the theoretical results. Third, the forces are independent of the thickness of the material if the thickness is greater than the penetration depth of the current. Three sets of four circular segments were used in the experimental analysis. The sets had thicknesses of 0.1524, 0.9525, and 1.2700 centimeters. The four segments have an average radius of 1.2152, 2.0335, 2.5792, and 3.3975 centimeters and each a width of 0.5456 centimeters. In each segment a slit of approximately 0.20 centimeters was made, and on each side of the slit a lead from a coaxial cable was attached.

To determine the natural frequency of the voltage induced in a segment, the High Energy Capacitor Discharge Unit was charged to 2 kilovolts and discharged into the hammer coil. This high intensity magnetic field induced a voltage in the segment which was observed on a 561A Tektronix Oscilloscope. A picture of this waveshape is shown in Figure 6 from which the frequency is approximately 3300 Hz. The damped sinusoidal waveform is similar to the waveform of the hammer coil shown in Figure 4.

The above procedure of inducing a voltage into a circular segment was repeated for each segment of the three sets of segments. The maximum induced voltage occurred at one-fourth the period and was observed for each segment. These experimental results are plotted in Figure 7. Given in Figure 8 is a plot of the theoretical values of the induced voltage per coil ampere as a function of the radial distance y . These particular values are for a material with a resistivity of 5.2×10^{-8} ohm-meters. From Figure 7 it can be seen that the experimental values of the induced voltage in the materials with thicknesses of 0.9525 and 1.2700 centimeters are approximately equal. Therefore, since the force

is directly proportional to the induced voltage, it is determined that the forces are independent of the thickness of the material if the thickness is greater than the penetration depth of the current. Also the plots of Figures 7 and 8 agree in that the voltage induced in the material of 0.1524 thickness is greater than voltage induced in the materials with a thickness greater than the penetration depth. Comparing the general shape of each curve in Figures 7 and 8, the definite similarity is easily seen.

Experimental error can be attributed to several causes. The center line of the circular segments and the center line of the coil were not matched exactly. The segment could not be placed flush against the hammer coil due to the coaxial cable. Voltage was induced in the connections of the cable. The circular segments could not be duplicated to the exact theoretical values.

y (Centimeters)	FORCE ($\times 10^{-4}$) (Newtons/Coil Ampere ²)	PRESSURE ($\times 10^{-1}$) (Newtons/Meter ² - Coil Ampere ²)	θ_F (Degrees)
0.2479	0.0000	0.0000	-175.41
0.7935	0.0293	0.1077	-162.38
1.3391	0.1714	0.3733	-141.98
1.8847	0.4066	0.6293	-124.33
2.4303	0.6749	0.8101	-111.90
2.9759	0.9498	0.9311	-100.27
3.5215	1.2102	1.0025	- 89.75
4.0671	1.4099	1.0112	- 79.29
4.6127	1.5230	0.9632	- 68.78
5.1583	1.2940	0.7318	- 50.78
5.7039	0.7843	0.4011	- 31.24
6.2495	0.4712	0.2199	- 22.38
6.7951	0.3073	0.1319	- 18.43
7.3407	0.2035	0.0809	- 15.74

Table 5. The Theoretical Values of Force, Pressure, and Resultant Angle as a Function of the Radial Distance y on Sheets of Materials with a Resistivity of 5.9 Microhm-Centimeters and Thicknesses of 0.9525, 1.2700, and 1.9050 Centimeters.

y (Centimeters)	FORCE ($\times 10^{-4}$) (Newtons/Coil Ampere ²)	PRESSURE ($\times 10^{-1}$) (Newtons/Meter ² - Coil Ampere ²)	θ_F (Degrees)
0.2479	0.0000	0.0000	-175.46
0.7935	0.0309	0.1134	-162.48
1.3391	0.1811	0.3944	-142.70
1.8847	0.4315	0.6678	-124.95
2.4303	0.7184	0.8622	-111.79
2.9759	1.0121	0.9921	-100.19
3.5215	1.2935	1.0715	- 89.74
4.0671	1.5039	1.0787	- 79.40
4.6127	1.6301	1.0309	- 69.08
5.1583	1.3900	0.7861	- 50.87
5.7039	0.8339	0.4265	- 30.97
6.2495	0.4986	0.2328	- 22.11
6.7951	0.3257	0.1398	- 18.21
7.3407	0.2162	0.0859	- 15.54

Table 6. The Theoretical Values of Force, Pressure, and Resultant Angle as a Function of the Radial Distance y on Sheets of Materials with a Resistivity of 5.4 Microhm-Centimeters and Thicknesses of 0.9525, 1.2700, and 1.9050 Centimeters.

y (Centimeters)	FORCE ($\times 10^{-4}$) (Newtons/Coil Ampere ²)	PRESSURE ($\times 10^{-1}$) (Newtons/Meter ² - Coil Ampere ²)	θ_F (Degrees)
0.2479	0.0000	0.0000	-175.48
0.7935	0.0316	0.1161	-162.54
1.3391	0.1858	0.4048	-142.71
1.8847	0.4432	0.6860	-124.87
2.4303	0.7372	0.8849	-111.72
2.9759	1.0396	1.0191	-100.15
3.5215	1.3308	1.1024	- 89.74
4.0671	1.5491	1.1111	- 79.46
4.6127	1.6828	1.0642	- 69.35
5.1583	1.4333	0.8105	- 50.66
5.7039	0.8536	0.4366	- 30.57
6.2495	0.5083	0.2373	- 22.07
6.7951	0.3316	0.1424	- 18.10
7.3407	0.2198	0.0874	- 15.45

Table 7. The Theoretical Values of Force, Pressure, and Resultant Angle as a Function of the Radial Distance y on Sheets of Materials with a Resistivity of 5.2 Microhm-Centimeters and Thicknesses of 0.9525, 1.2700, and 1.9050 Centimeters.

y (Centimeters)	FORCE ($\times 10^{-4}$) (Newtons/Coil Ampere ²)	PRESSURE ($\times 10^{-1}$) (Newtons/Meter ² - Coil Ampere ²)	θ_F (Degrees)
0.2479	0.0000	0.0000	-175.61
0.7935	0.0369	0.1355	-162.84
1.3391	0.2182	0.4754	-142.68
1.8847	0.5219	0.8077	-124.52
2.4303	0.8684	1.0424	-111.42
2.9759	1.2300	1.2057	- 99.96
3.5215	1.5821	1.3106	- 89.75
4.0671	1.8523	1.3285	- 79.77
4.6127	2.0393	1.2897	- 70.12
5.1583	1.7271	0.9767	- 51.21
5.7039	0.9975	0.5101	- 30.14
6.2495	0.5854	0.2732	- 21.32
6.7951	0.3813	0.1637	- 17.58
7.3407	0.2522	0.1002	- 14.96

Table 8. The Theoretical Values of Force, Pressure, and Resultant Angle as a Function of the Radial Distance y on Sheets of Materials with a Resistivity of 4.0 Microhm-Centimeters and Thicknesses of 0.9525, 1.2700, and 1.9050 Centimeters.

y (Centimeters)	FORCE ($\times 10^{-4}$) (Newtons/Coil Ampere ²)	PRESSURE ($\times 10^{-1}$) (Newtons/Meter ² - Coil Ampere ²)	θ_F (Degrees)
0.2479	0.0000	0.0000	-176.23
0.7935	0.0241	0.0887	-164.36
1.3391	0.1483	0.3230	-142.59
1.8847	0.3592	0.5560	-122.60
2.4303	0.5946	0.7137	-109.78
2.9759	0.8586	0.8416	- 99.00
3.5215	1.1218	0.9293	- 90.17
4.0671	1.3797	0.9896	- 81.80
4.6127	1.6393	1.0367	- 76.49
5.1583	1.3637	0.7712	- 54.62
5.7039	0.6812	0.3484	- 26.72
6.2495	0.3701	0.1727	- 18.08
6.7951	0.2421	0.1039	- 14.95
7.3407	0.1599	0.0635	- 12.55

Table 9. The Theoretical Values of Force, Pressure, and Resultant Angle as a Function of the Radial Distance y on Sheets of Materials with a Resistivity of 5.9 Microhm-Centimeters and a Thickness of 0.1524 Centimeters.

y (Centimeters)	FORCE ($\times 10^{-4}$) (Newtons/Coil Ampere ²)	PRESSURE ($\times 10^{-1}$) (Newtons/Meter ² - Coil Ampere ²)	θ_F (Degrees)
0.2479	0.0000	0.0000	-176.23
0.7935	0.0264	0.0969	-164.36
1.3391	0.1620	0.3529	-142.59
1.8847	0.3925	0.6075	-122.60
2.4303	0.6496	0.7798	-109.78
2.9759	0.9381	0.9195	- 99.00
3.5215	1.2257	1.0153	- 90.17
4.0671	1.5075	1.0813	- 81.80
4.6127	1.7911	1.1327	- 76.49
5.1583	1.4900	0.8426	- 54.62
5.7039	0.7442	0.3806	- 26.72
6.2495	0.4043	0.1887	- 18.08
6.7951	0.2645	0.1136	- 14.95
7.3407	0.1747	0.0694	- 12.55

Table 10. The Theoretical Values of Force, Pressure, and Resultant Angle as a Function of the Radial Distance y on Sheets of Materials with a Resistivity of 5.4 Microhm-Centimeters and a Thickness of 0.1524 Centimeters.

y (Centimeters)	FORCE ($\times 10^{-4}$) (Newtons/Coil Ampere ²)	PRESSURE ($\times 10^{-1}$) (Newtons/Meter ² - Coil Ampere ²)	θ_F (Degrees)
0.2479	0.0000	0.0000	-176.23
0.7935	0.0274	0.1006	-164.36
1.3391	0.1682	0.3664	-142.59
1.8847	0.4076	0.6308	-122.60
2.4303	0.6746	0.8098	-109.78
2.9759	0.9741	0.9549	- 99.00
3.5215	1.2728	1.0544	- 90.17
4.0671	1.5655	1.1228	- 81.80
4.6127	1.8600	1.1763	- 76.49
5.1583	1.5473	0.8751	- 54.62
5.7039	0.7729	0.3953	- 26.72
6.2495	0.4199	0.1960	- 18.08
6.7951	0.2747	0.1179	- 14.95
7.3407	0.1814	0.0721	- 12.55

Table 11. The Theoretical Values of Force, Pressure, and Resultant Angle as a Function of the Radial Distance y on Sheets of Materials with a Resistivity of 5.2 Microhm-Centimeters and a Thickness of 0.1524 Centimeters.

y (Centimeters)	FORCE ($\times 10^{-4}$) (Newtons/Coil Ampere ²)	PRESSURE ($\times 10^{-1}$) (Newtons/Meter ² - Coil Ampere ²)	θ_F (Degrees)
0.2479	0.0000	0.0000	-176.23
0.7935	0.0356	0.1308	-164.36
1.3391	0.2187	0.4764	-142.59
1.8847	0.5298	0.8201	-122.60
2.4303	0.8770	1.0527	-109.78
2.9759	1.2664	1.2414	- 99.00
3.5215	1.6547	1.3707	- 90.17
4.0671	2.0351	1.4597	- 81.80
4.6127	2.4180	1.5292	- 76.49
5.1583	2.0115	1.1376	- 54.62
5.7039	1.0047	0.5139	- 26.72
6.2495	0.5459	0.2548	- 18.08
6.7951	0.3571	0.1533	- 14.95
7.3407	0.2358	0.0937	- 12.55

Table 12. The Theoretical Values of Force, Pressure, and Resultant Angle as a Function of the Radial Distance y on Sheets of Materials with a Resistivity of 4.0 Microhm-Centimeters and a Thickness of 0.1524 Centimeters.

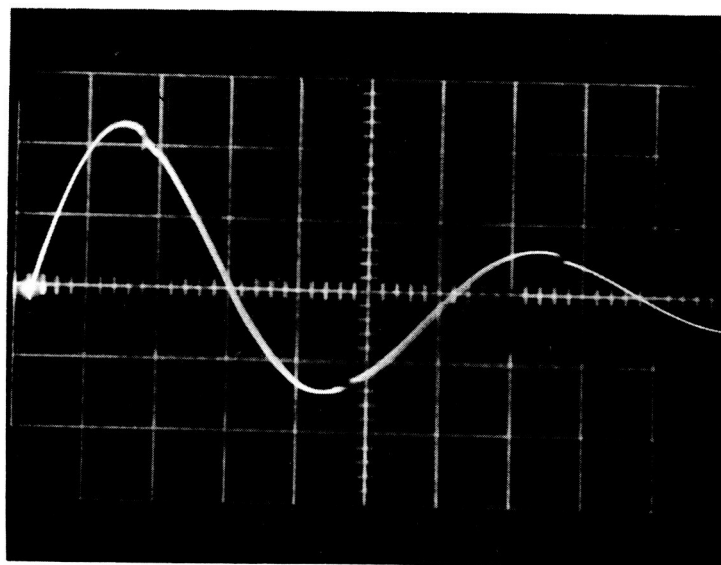


Figure 6. The Waveform of an Induced Voltage in an Actual Circular Segment as a Function of Time. (20 Volts/Centimeter and 50 Microseconds/Centimeter.)

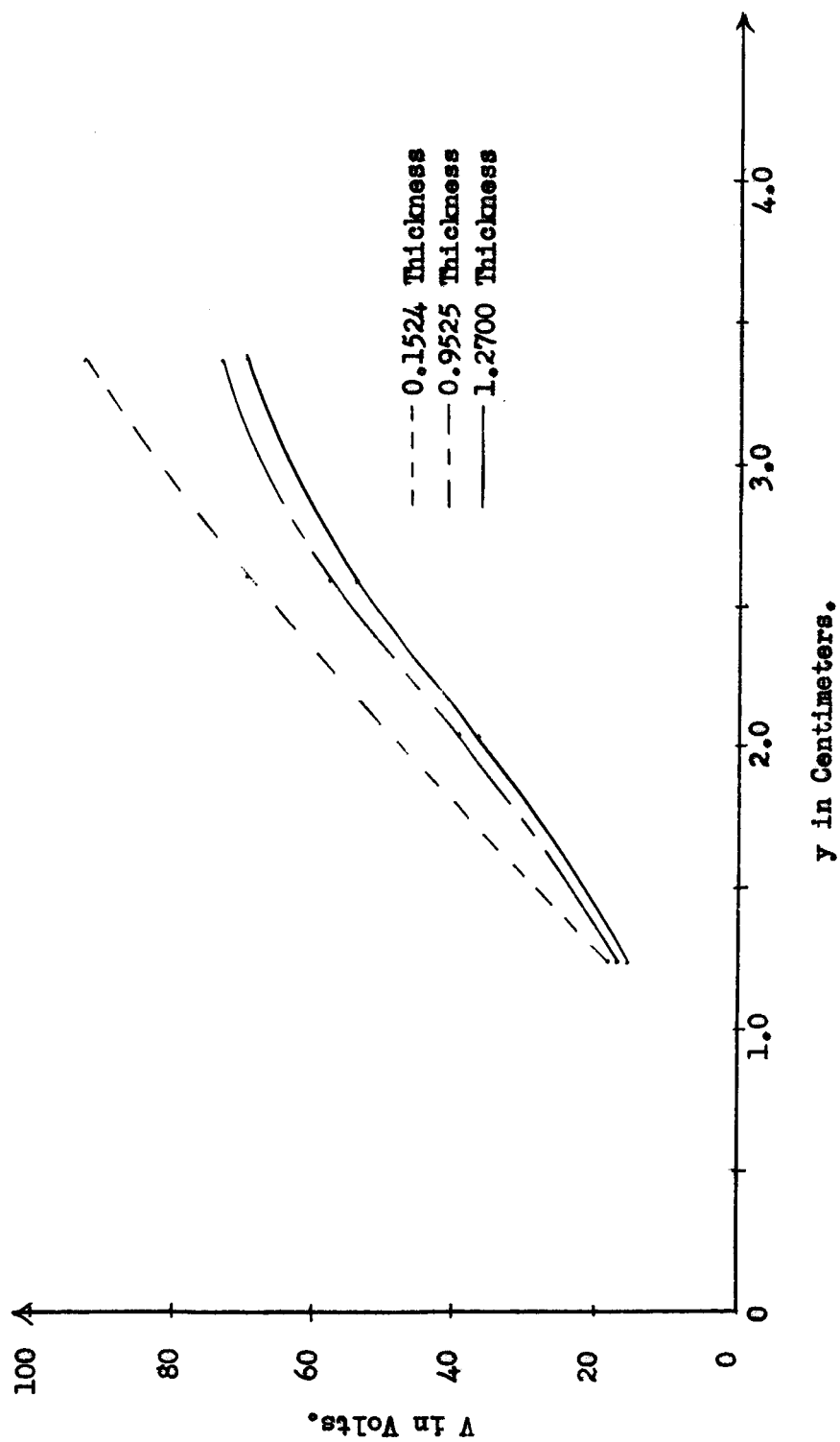


Figure 7. A Plot of the Experimental Data of an Induced Voltage V in the Actual Circular Segments as a Function of the Radial Distance y . (Capacitor Discharge Unit Charged to 2 Kilovolts.)

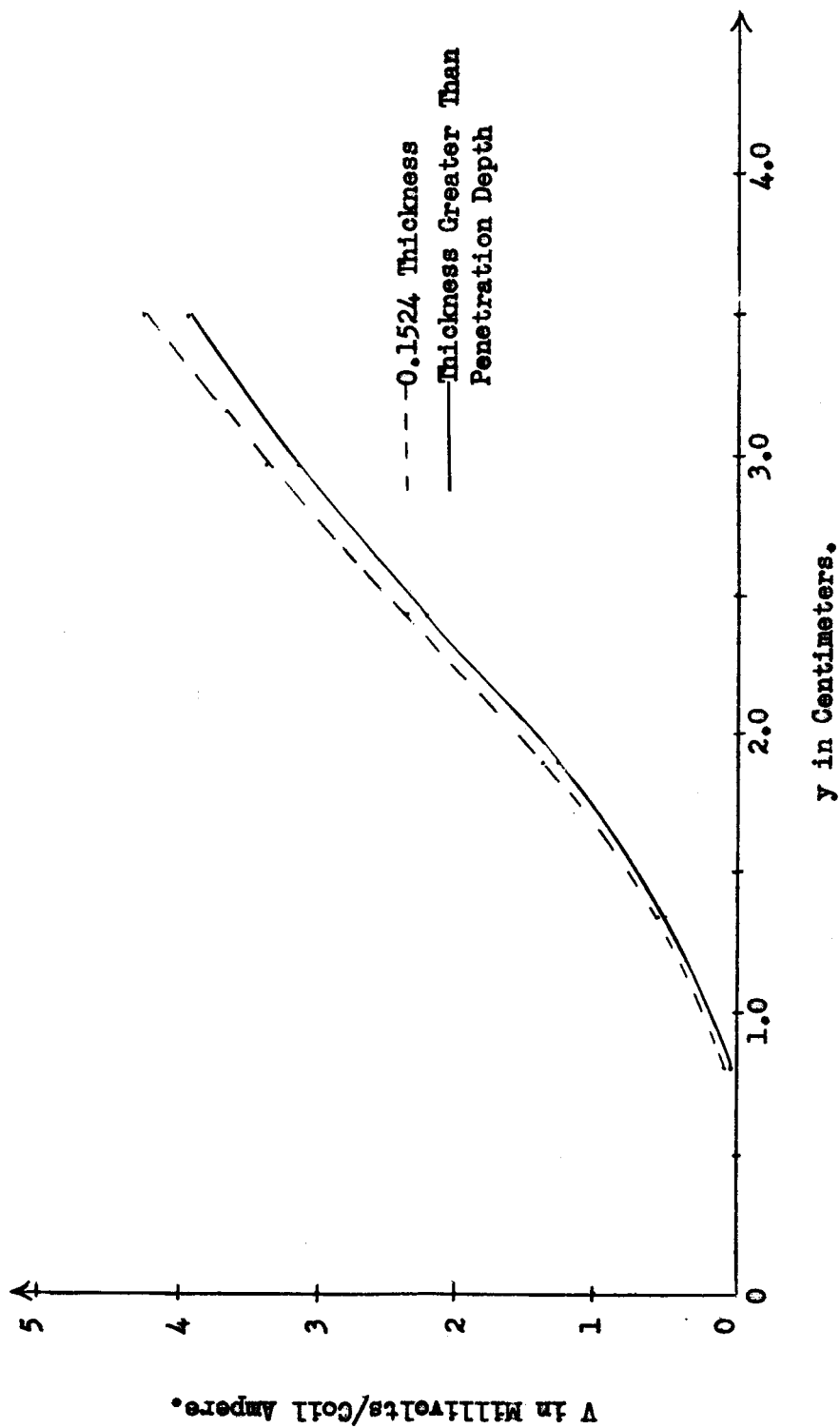


Figure 8. A Plot of the Theoretical Values of an Induced Voltage per Coil Ampere as a Function of the Radial Distance y . (For Material with Resistivity of 5.2×10^{-8} Ohm-Meters.)

CHAPTER V

CONCLUSION

The purpose of this study was to determine the maximum static forces on sheets of metallic materials due to magnetomotive forming. The materials studied were a combination of four different thicknesses and of six different aluminum alloys.

These forces were calculated by assuming the material to be made up of concentric circular segments having the same center line as the hammer coil. The induced voltage was determined in each segment using Faraday's law. Then from a form of Lorentz's force equation the maximum force on each segment was calculated. With the hammer coil having a diameter of 10.3175 centimeters the maximum force was found to occur at points 4.6127 centimeters radially out from the center line of the coil. The values of force were found to vary inversely to the values of resistivity. The forces were also found to be independent of the thickness of the material if the thickness is greater than the penetration depth of the current.

The theoretical results of this study were verified by actually measuring the induced voltage in circular segments of different thicknesses. Also, the assumed natural frequency was found to be correct by observing the waveshape of the induced voltage on an oscilloscope.

The next step in the study of the hammer coil should be to determine what happens as the plate becomes decoupled from the coil. The term decoupled, as used here, is synonymous with the plate being deformed by moving away from the surface of the coil. In such a study,

the mechanical properties of the material would have to be considered as well as its electrical characteristics. The motion of the material in a magnetic field would produce induced voltages due to motion which were not considered in this study. The magnitude of the voltage due to motion would depend both on the strength of the magnetic field and on the speed of movement of the material.

The measured voltage induced in the circular segments indicated that a peak current of approximately 20,000 amperes was flowing in the hammer coil. This calculation was made by a comparison of Figure 8 and Figure 9. No method was devised to verify these results experimentally.

APPENDIX A

```

C   HAMMER COIL VECTOR MAGNETIC POTENTIAL DETERMINATION
C   NEAR FIELD
    DIMENSION SSS(11), W(11)
    DIMENSION VMP(22,28)
    READ 50, IS
50  FORMAT(12)
    DO 11 I = 1,11
      P = I-1
11  SSS(I) = SIN(3.14159/2.-P*3.14159/10.)
    DO 55 N = IS,28
      V = N
      FN=N/2
      NFN=FN*2.
      IF(NFN-N)12,13,99
12  ZPP = .075
      GO TO 14
13  ZPP = .025
14  Y = 0.0976+.1074*(V-1.)
      DO 55 MM = 1,11
        M = MM
        WW = M
        Z = ZPP+.100*(WW-1.)
        IF(NFN-N)15,16,99
15  M = 2*M
        GO TO 17
16  M = (2*M)-1
17  A = .4792
        PRINT 10, Y, Z
10  FORMAT(2F10.4)
        ZP = Z
        VMPP = 0.
        COUNT = 0.
        DO 22 J = 1,45
          Q = J
          IF(COUNT-3.) 4,3,99
3    COUNT = 1.
          A = A+.0594
          GO TO 9
4    COUNT = COUNT+1.
          A = A+.0240
9    DO 33 K = 1,10
        U = K
        Z = ZP+.0500*(U-1.)
        R = (Y*Y+Z*Z)**.5
        THETA = 1.570796-ATAN(2/Y)
        R2A2 = R*R + A*A
        TWORA = 2.*R*A*SIN(THETA)
        DO 44 L = 1,11
44  W(L) = SSS(L)/((R2A2-TWORA*SSS(L))**.5)

```



```

WCOMP1 = 0.
WCOMP2 = 0.
WCOMP1 = W(2) + W(4) + W(6) + W(8) + W(10)
WCOMP1 = 4.*WCOMP1
WCOMP2 = W(3) + W(5) + W(7) + W(9)
WCOMP2 = 2.*WCOMP2
VMPI = (W(1) + W(11) + WCOMP1 + WCOMP2)*A
VMPP = VMPP + VMPI
33 CONTINUE
22 CONTINUE
  VMP(M,N) = VMPP*(1./1800.)
  PRINT 20, VMP(M,N)
20 FORMAT(E18.6)
55 CONTINUE
  PRINT 40
40 FORMAT(5X,1HY,9X,1HZ,12X,2HHY,12X,2HHZ,10X,5HHRSLT,6X,5HTHETA)
  ISS = IS + 1
  DO 77 J = ISS,27
    E = J
    XFN = J/2
    NFX = XFN*2.
    IF(NFX-J)23,24,99
23 ZPPP = .125
    GO TO 25
24 ZPPP = .075
25 Y = .2050 + .1074*(E-2.)
    DO 77 KK = 1,10
      K = KK
      F = K
      Z = ZPPP + .100*(F-1.)
      IF(NFX-J)26,27,99
26 K = (2*K) + 1
      GO TO 28
27 K = 2*K
28 HY = (VMP(K-1,J)-VMP(K+1,J))*393.7
      HZ = (VMP(K,J+1)-VMP(K,J-1))*183.3
      HRSLT = (HY*HY + HZ*HZ)**.5
      THETA = ATANF(HZ/HY)
      THETA = THETA*(180./3.14159)
      PRINT 30, Y, Z, HY, HZ, HRSLT, THETA
30 FORMAT(2F10.4,3E14.8,F10.4//)
77 CONTINUE
99 STOP
END

```

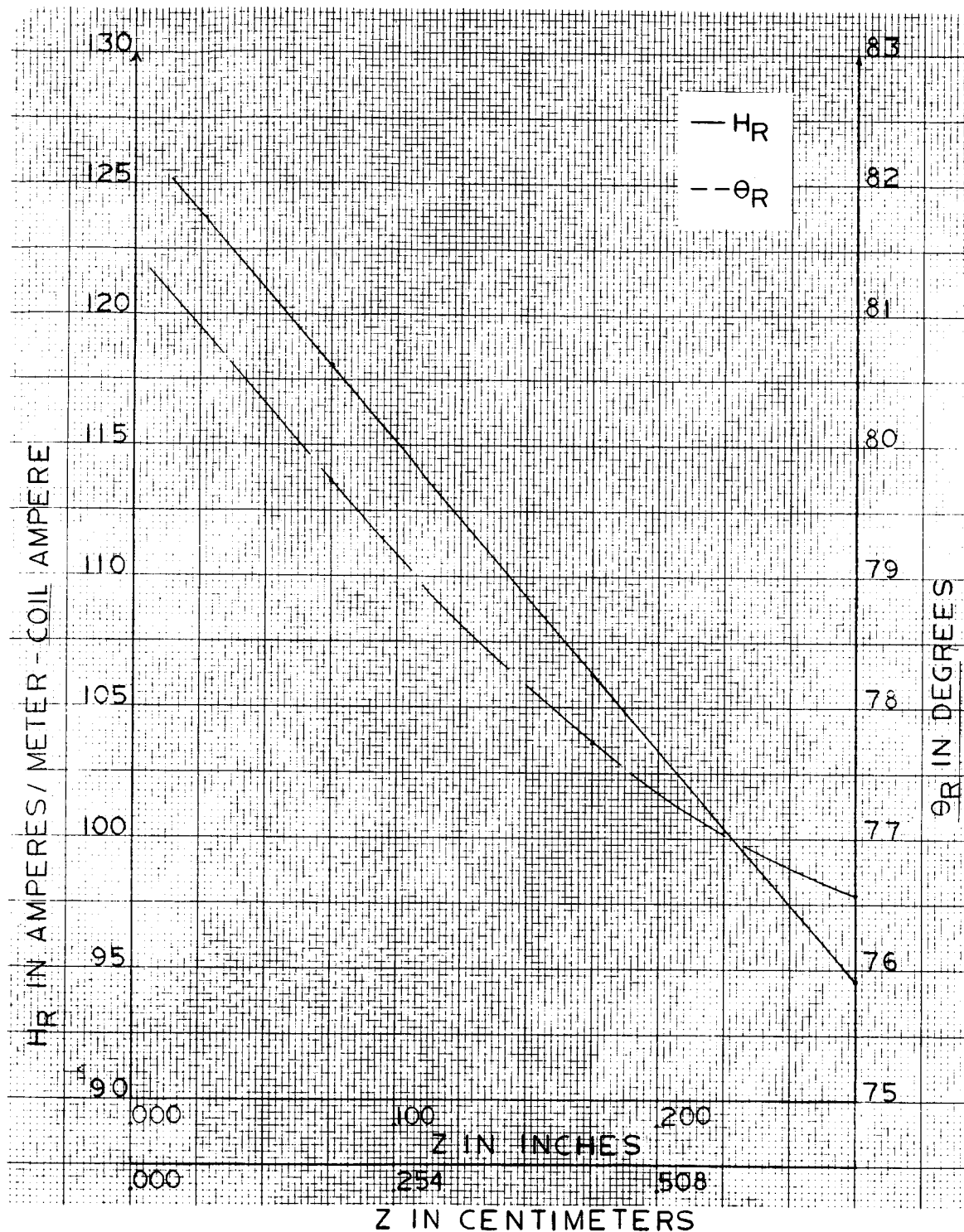


Figure B-1. A Plot of the Magnetic Field Intensity and the Resultant Angle as a Function of the Distance Normal to the Surface of the Hammer Coil for a Constant Radial Value, y , of 0.5207 Centimeters.

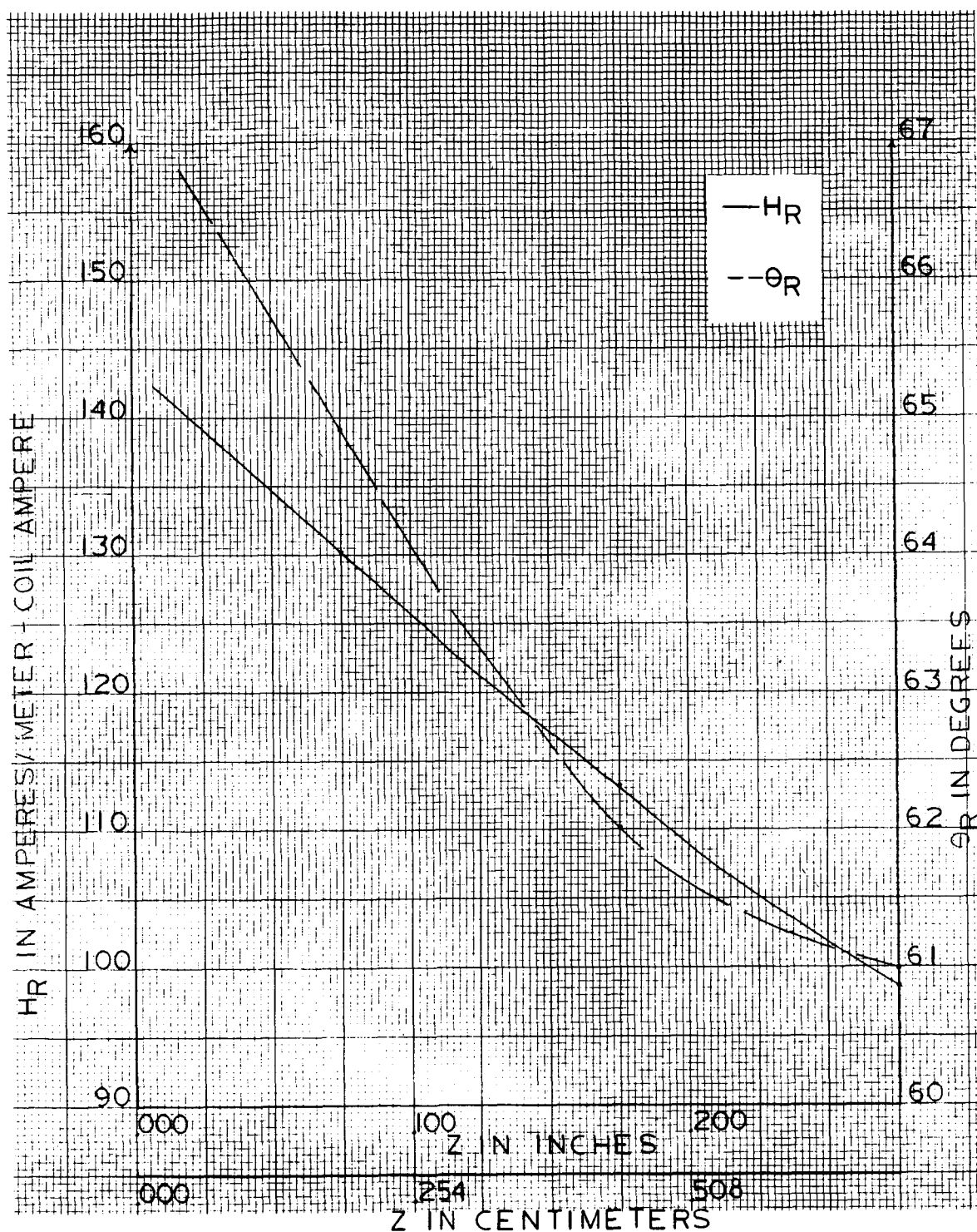


Figure B-2. A Plot of the Magnetic Field Intensity and the Resultant Angle as a Function of the Distance Normal to the Surface of the Hammer Coil for a Constant Radial Value, y , of 1.0663 Centimeters.

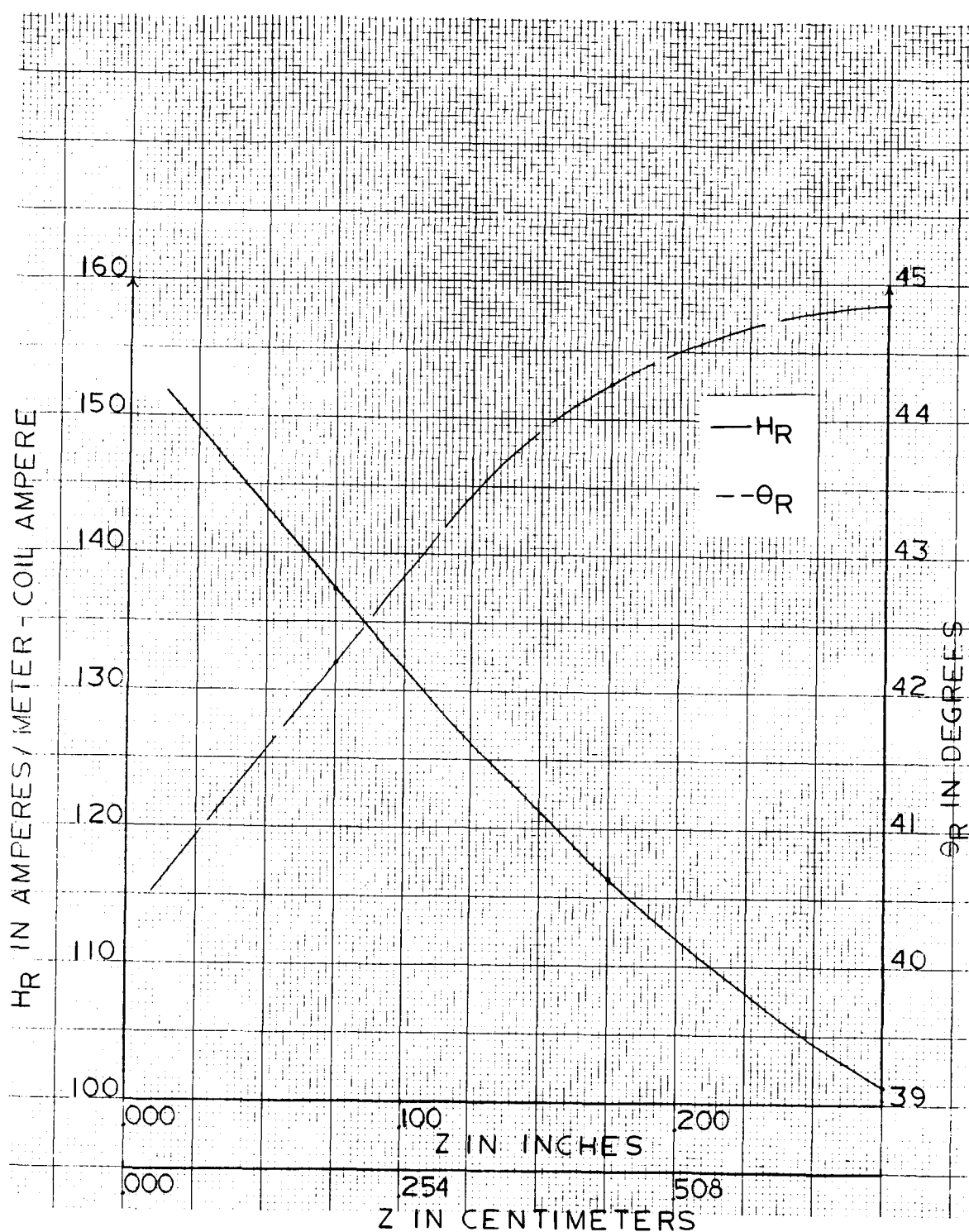


Figure B-3. A Plot of the Magnetic Field Intensity and the Resultant Angle as a Function of the Distance Normal to the Surface of the Hammer Coil for a Constant Radial Value, y , of 1.6119 Centimeters.

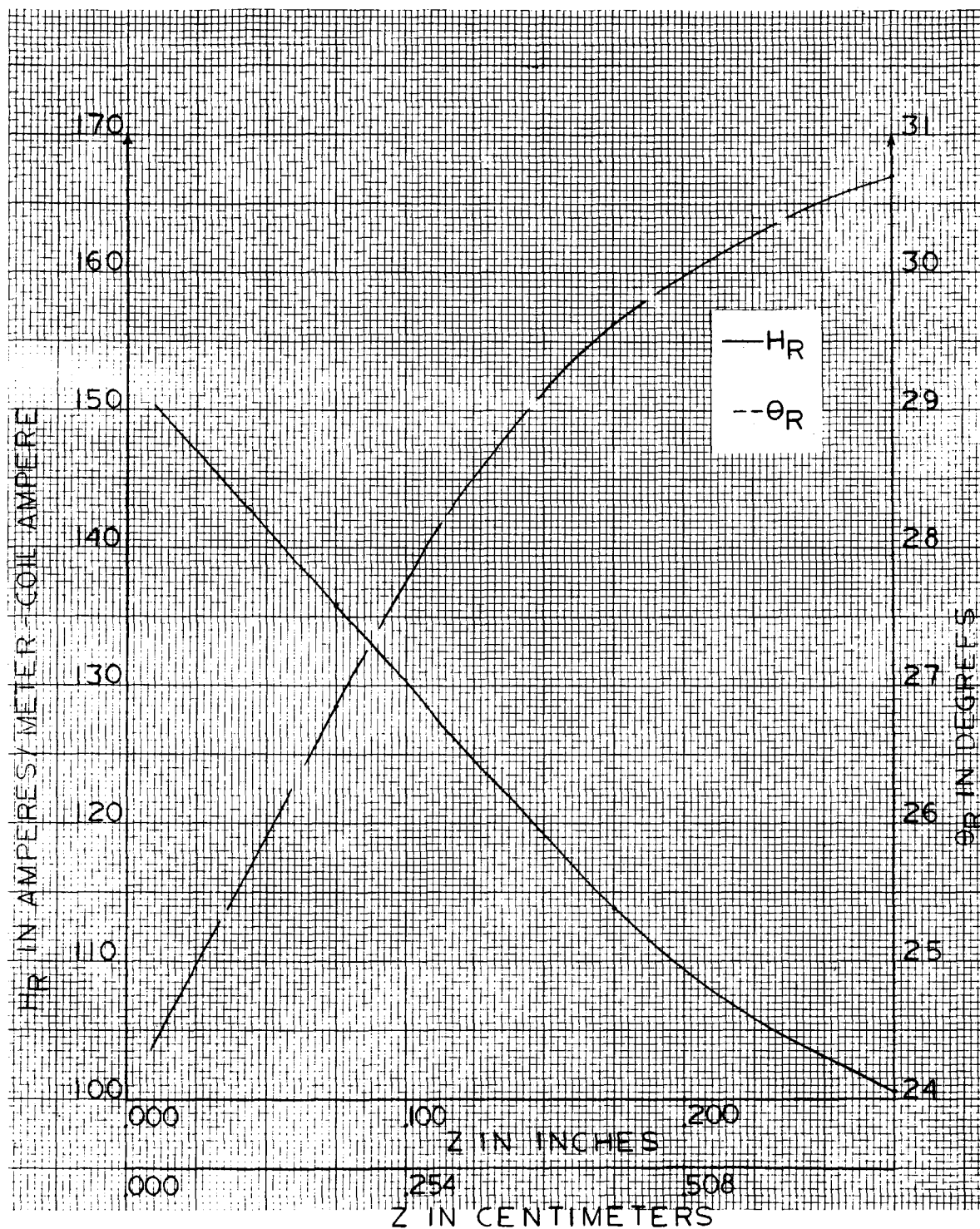


Figure B-4. A Plot of the Magnetic Field Intensity and the Resultant Angle as a Function of the Distance Normal to the Surface of the Hammer Coil for a Constant Radial Value, y , of 2.1575 Centimeters.

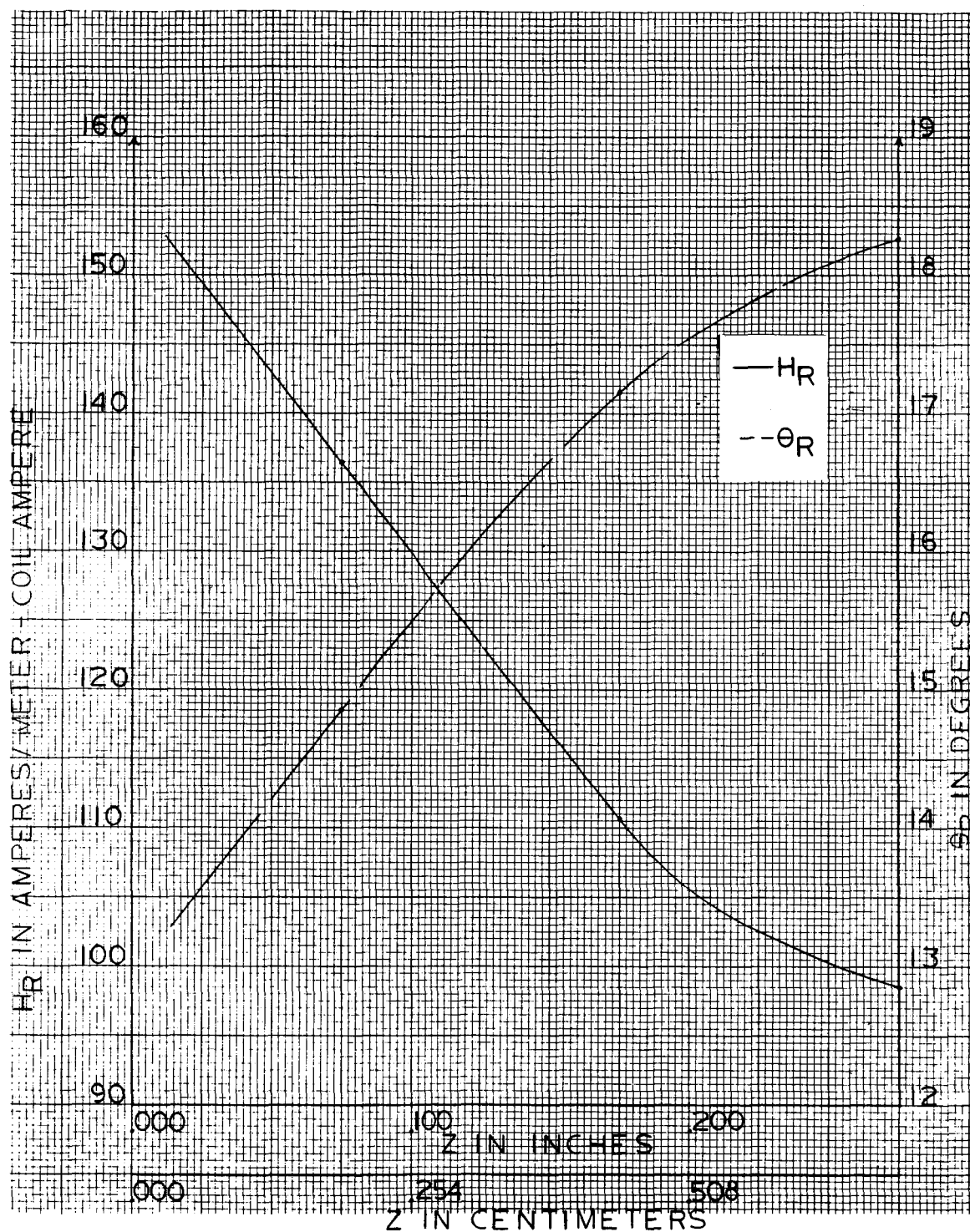


Figure B-5. A Plot of the Magnetic Field Intensity and the Resultant Angle as a Function of the Distance Normal to the Surface of the Hammer Coil for a Constant Radial Value, y , of 2.7031 Centimeters.

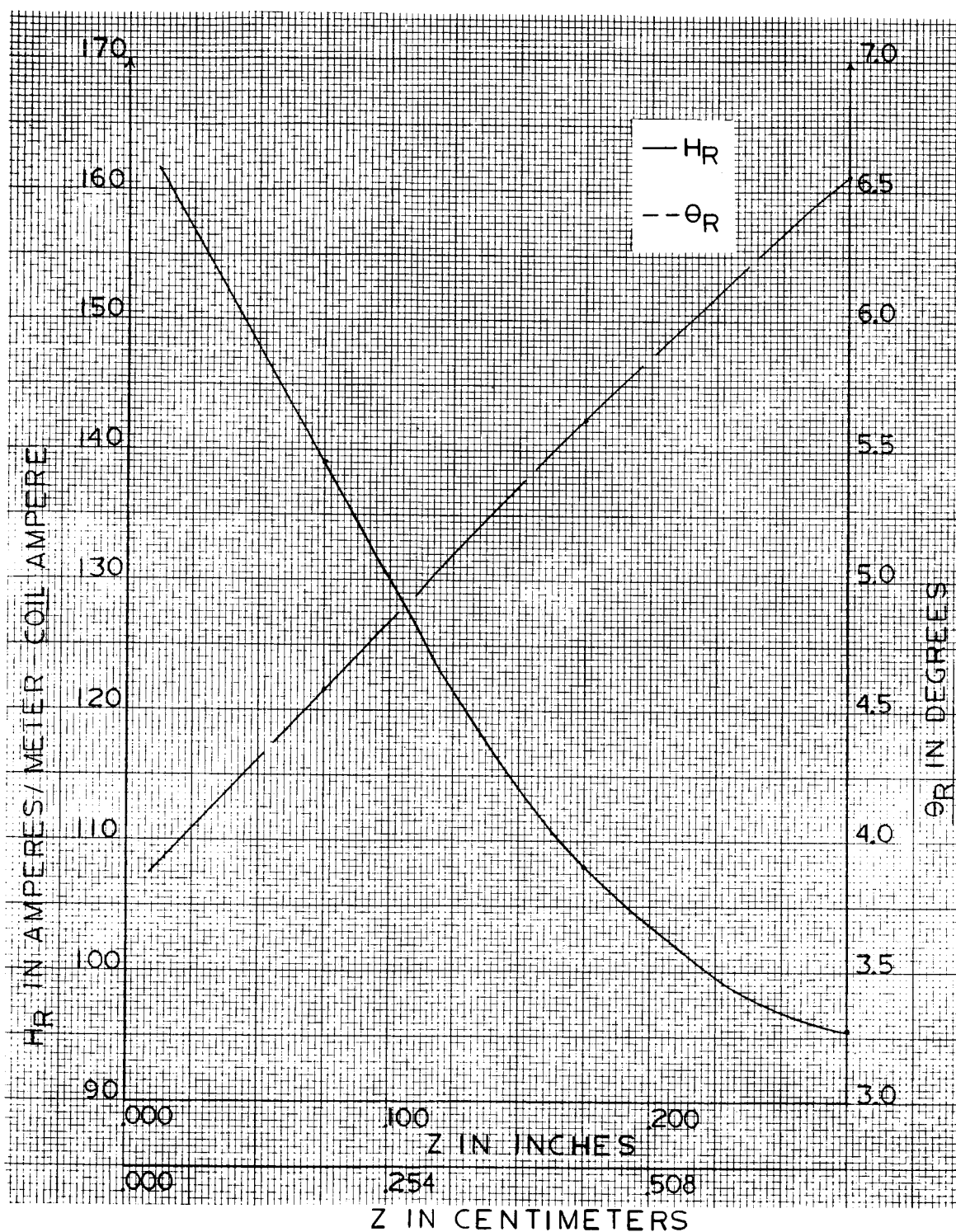


Figure B-6. A Plot of the Magnetic Field Intensity and the Resultant Angle as a Function of the Distance Normal to the Surface of the Hammer Coil for a Constant Radial Value, y , of 3.2487 Centimeters.

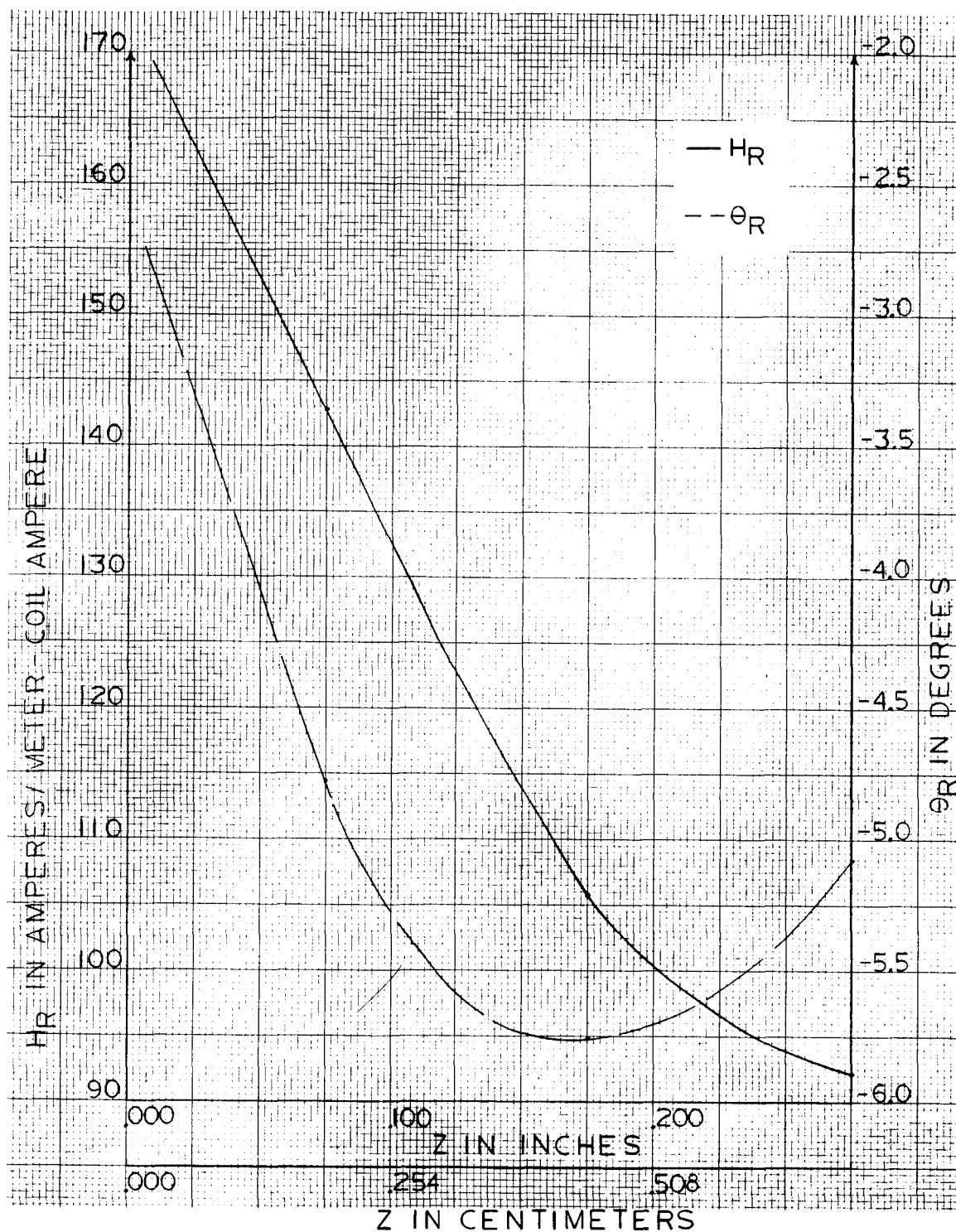


Figure B-7. A Plot of the Magnetic Field Intensity and the Resultant Angle as a Function of the Distance Normal to the Surface of the Hammer Coil for a Constant Radial Value, y , of 3.7943 Centimeters.

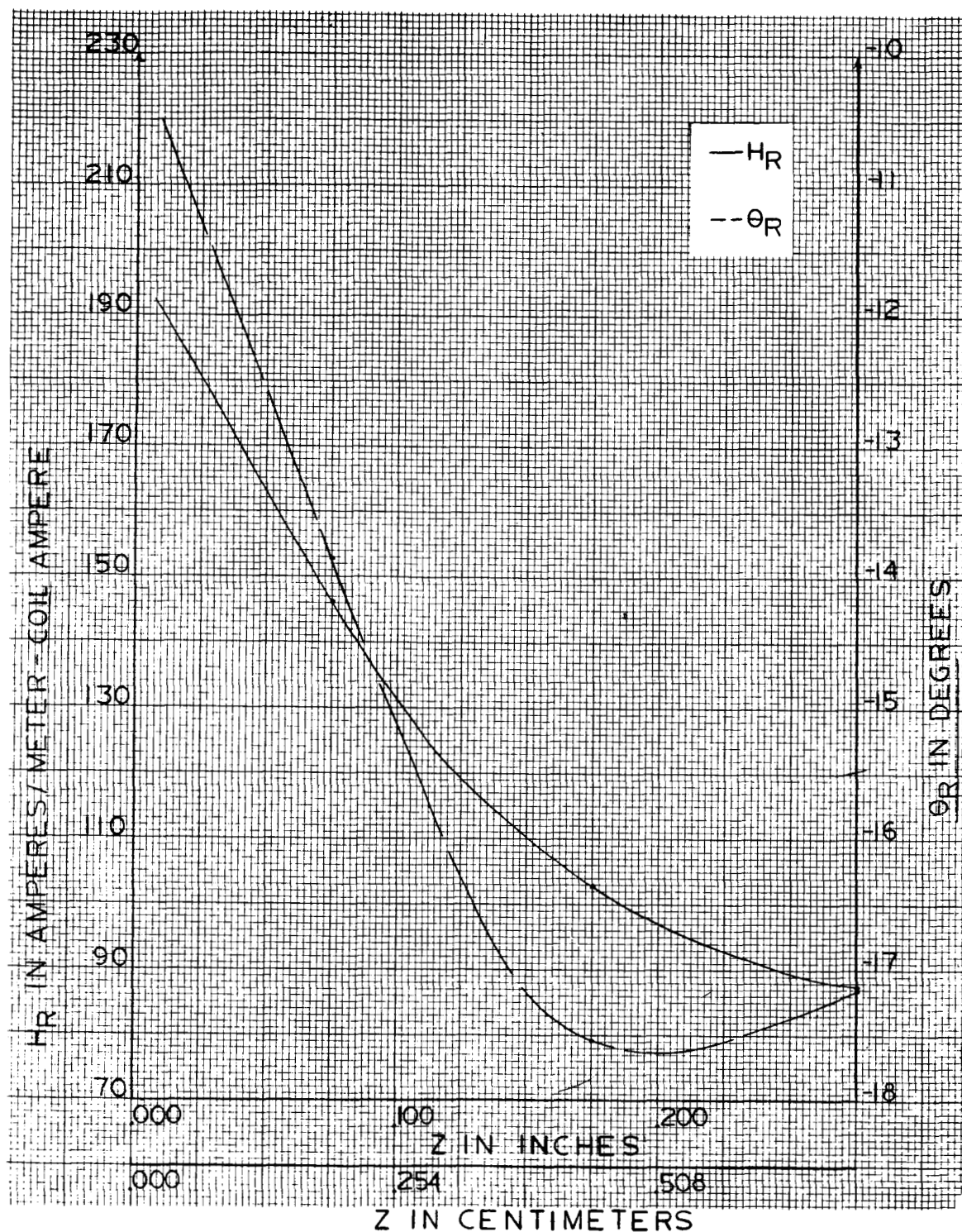


Figure B-8. A Plot of the Magnetic Field Intensity and the Resultant Angle as a Function of the Distance Normal to the Surface of the Hammer Coil for a Constant Radial Value, y , of 4.3398 Centimeters.

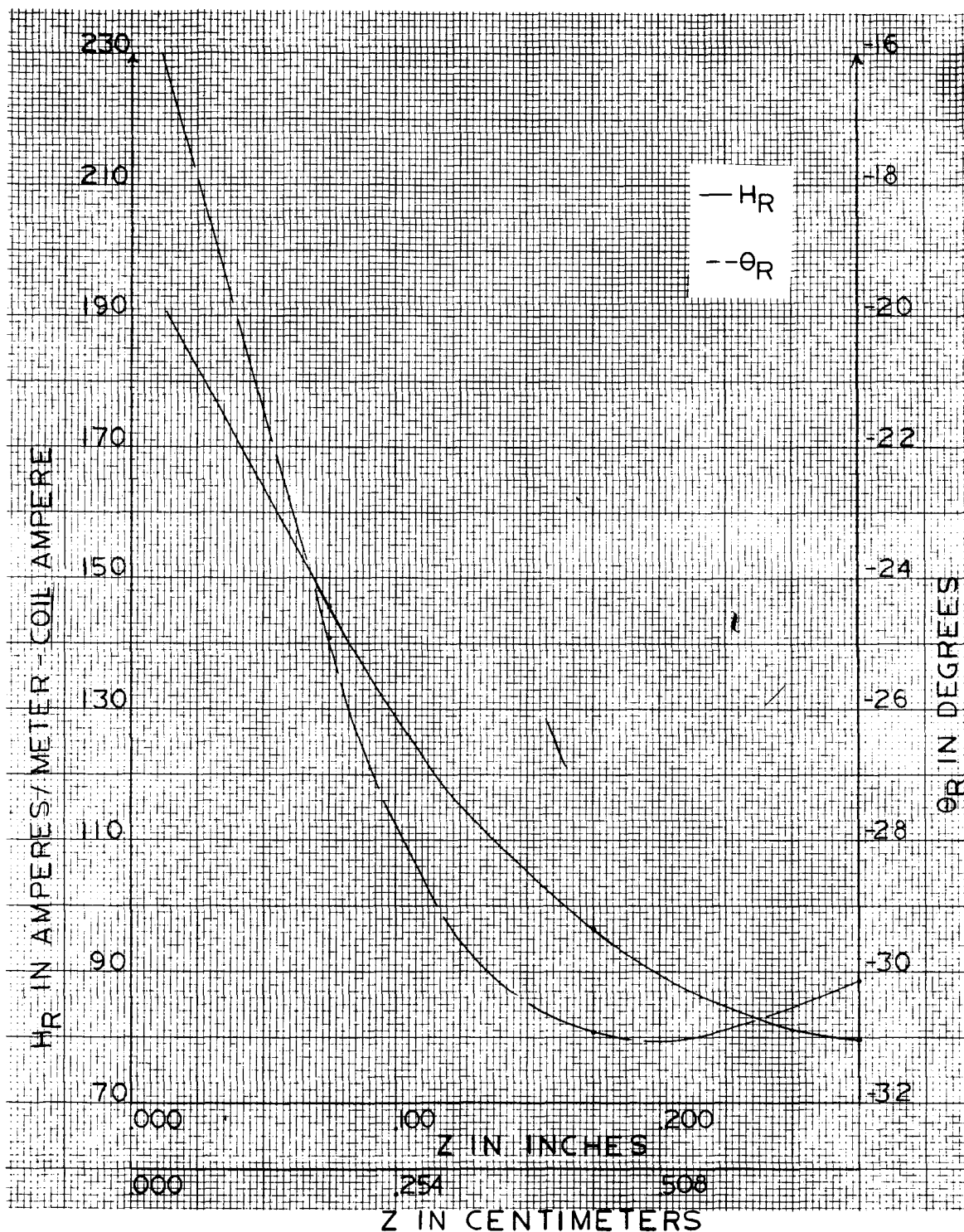


Figure B-9. A Plot of the Magnetic Field Intensity and the Resultant Angle as a Function of the Distance Normal to the Surface of the Hammer Coil for a Constant Radial Value, y , of 4.8854 Centimeters.

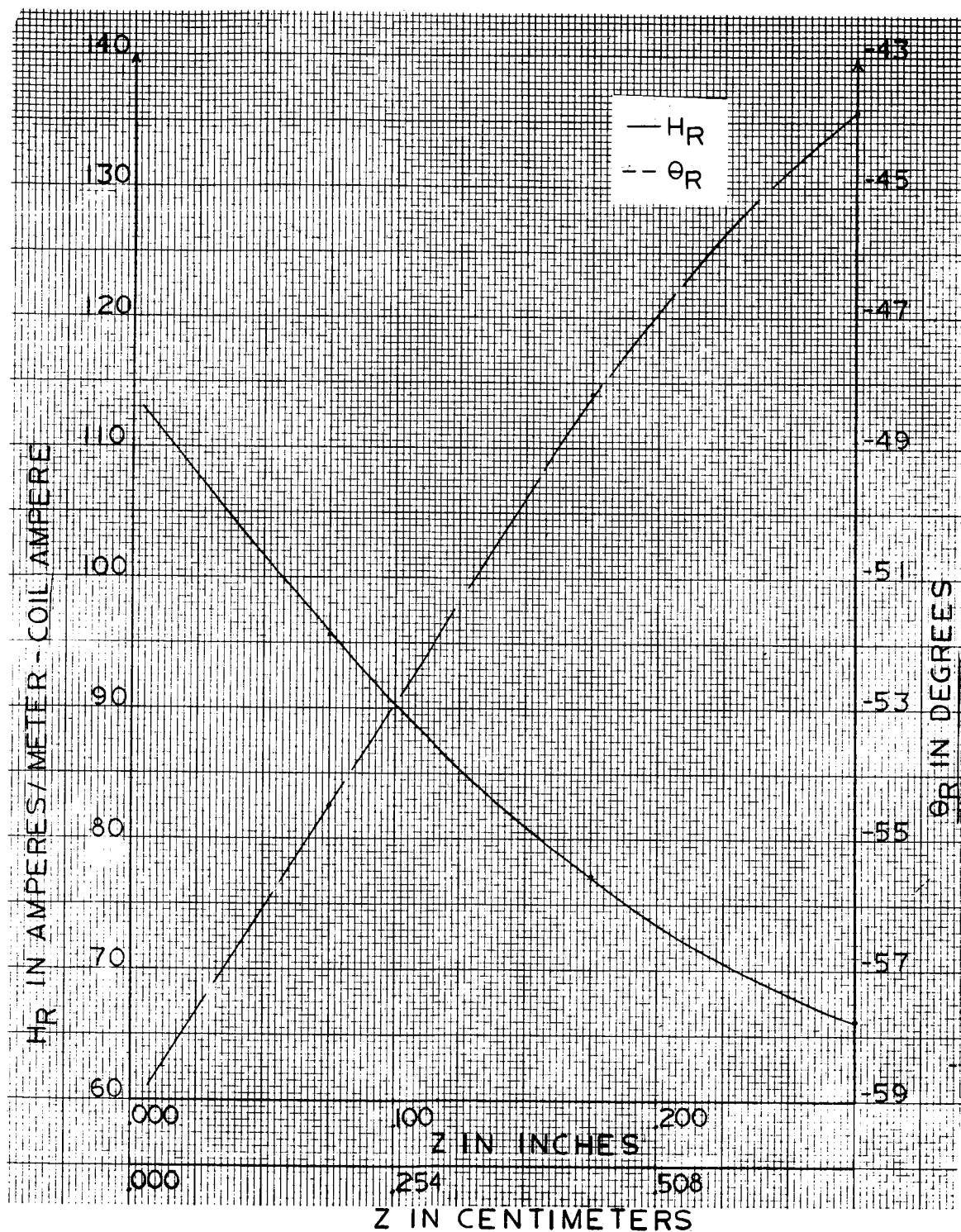


Figure B-10. A Plot of the Magnetic Field Intensity and the Resultant Angle as a Function of the Distance Normal to the Surface of the Hammer Coil for a Constant Radial Value, y , of 5.4310 Centimeters.

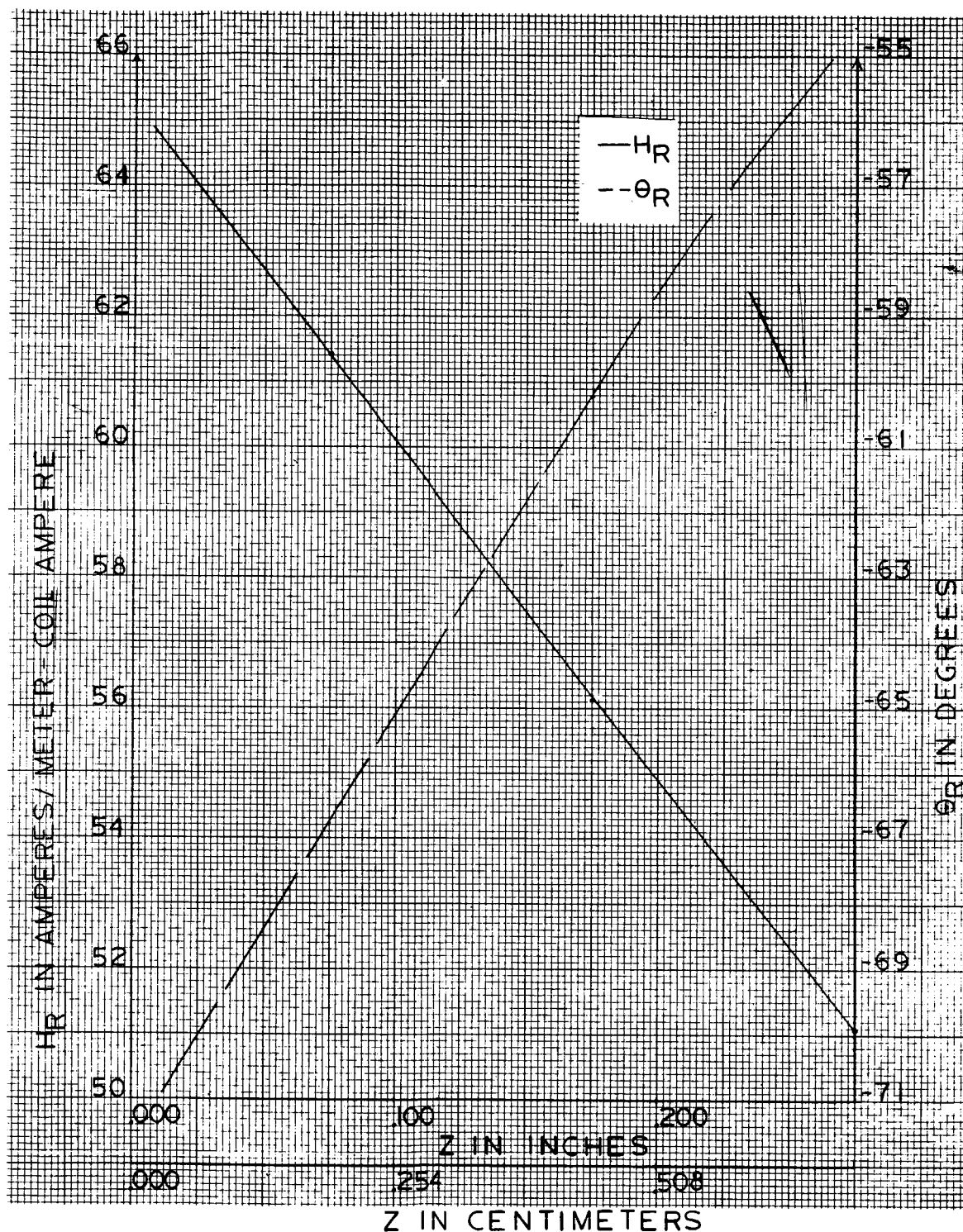


Figure B-11. A Plot of the Magnetic Field Intensity and the Resultant Angle as a Function of the Distance Normal to the Surface of the Hammer Coil for a Constant Radial Value, y , of 5.9766 Centimeters.

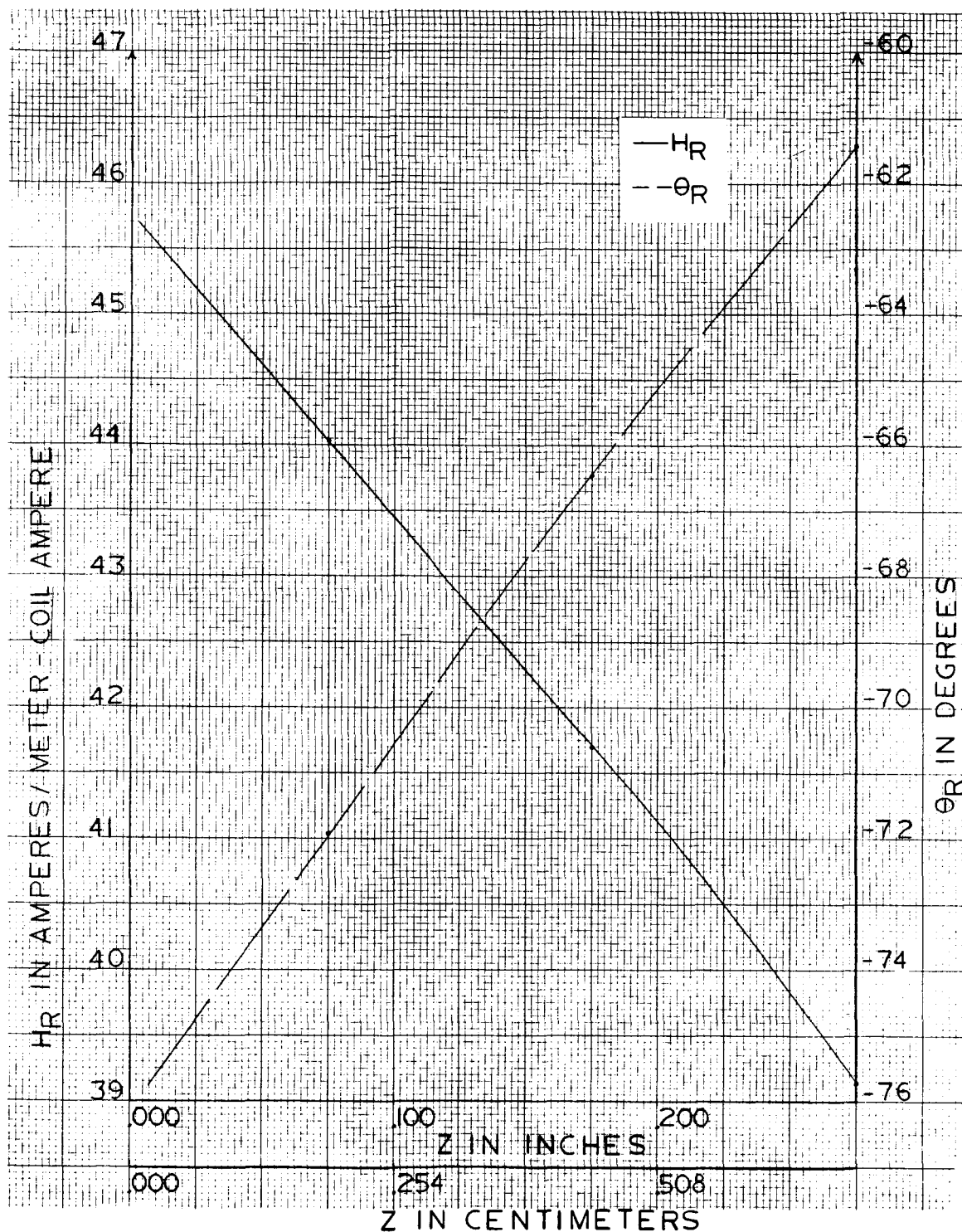


Figure B-12. A Plot of the Magnetic Field Intensity and the Resultant Angle as a Function of the Distance Normal to the Surface of the Hammer Coil for a Constant Radial Value, y , of 6.5222 Centimeters.

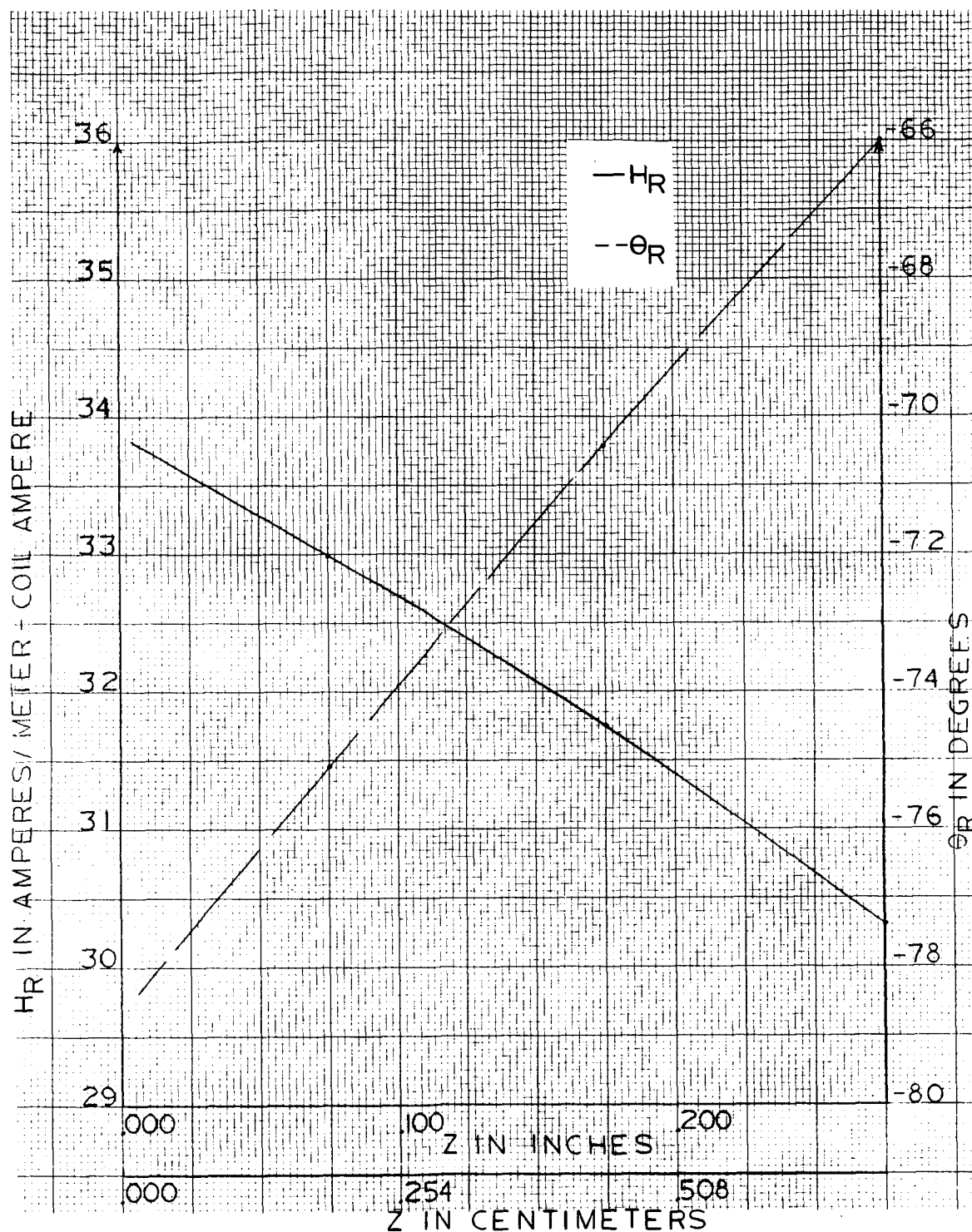


Figure B-13. A Plot of the Magnetic Field Intensity and the Resultant Angle as a Function of the Distance Normal to the Surface of the Hammer Coil for a Constant Radial Value, y , of 7.0678 Centimeters.

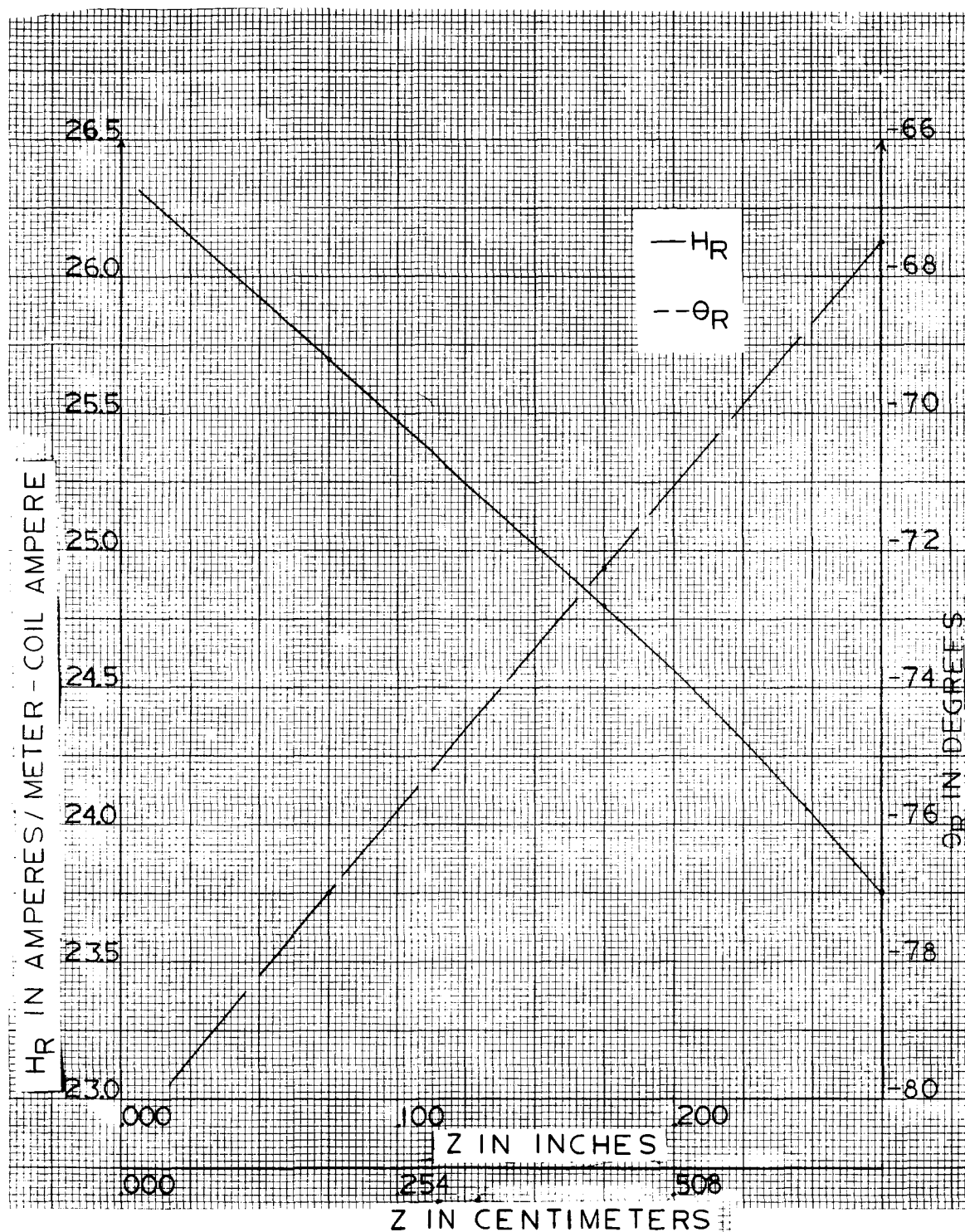


Figure B-14. A Plot of the Magnetic Field Intensity and the Resultant Angle as a Function of the Distance Normal to the Surface of the Hammer Coil for a Constant Radial Value, y , of 7.6134 Centimeters.

APPENDIX C

```

C C HAMMER COIL - FORCE AND PRESSURE PER AMPERE SQUARED
  DOUBLE PRECISION Z,Y2,B0,A1,R2,C2,HR2,Y12,B00,HZ2,HR12,HZ12,BZA1,
  1FLUX2,PRESS2,A,Y3,T1,A2,E1,RHO,TH2,Y22,T12,HZ3,HR22,HZ22,BZA2,
  2PHI1,PHI2,FORCE1,H,B2,T2,AT,E2,HR1,HR3,B22,T22,SA1,TH12,HZA1,DIA1,
  1DELTA,FORCE2,Y1,B1,T3,R1,C1,TH1,TH3,B11,HZ1,SA2,TH22,HZA2,DIA2,
  1FLUX1,PRESS1
  1 READ(1,11) RHO, DELTA, Z
  11 FORMAT (2D10.4, F10.0 )
    A = 0.
    H = .5456
    WRITE ( 3,35) RHO , DELTA , Z
  35 FORMAT ( 1H1, 4X, 3HRHO, 12X, 5HDELTA, 12X, 1HZ //2E15.4, F15.6//
    14X, 1HY, 10X, 17HFORCE(NEW/AMP**2), 8X, 8HPRESSURE, 12X,
    23HPHI//)
    IF (Z - 4.) 2, 99, 99
  2 READ (1, 10 ) HR1, TH1, Y1, HR2, TH2, Y2, HR3, TH3, Y3
  10 FORMAT ( 3F10.0, 42X )
    B2 = (HR3 - 2.*HR2 + HR1)/ (2. * H**2 )
    B1 = (-B2 *(2.*Y1*H + H*H) + HR2 - HR1)/H
    B0 = HR1 - (B2 * Y1*Y1 + B1 * Y1 )
    Y12 = (Y2 - H/2.)
    HR12 = B0 + B1*Y12 + B2 * Y12**2
    Y22 = ( Y2 + H/2.)
    HR22 = B0 + B1* Y22 + B2* Y22**2
    B22 = (TH3 - 2.*TH2 + TH1)/( 2.* H**2)
    B11 = (-B22*( 2.*Y1* H + H*H) + TH2 -TH1)/H
    B00 = TH1 - (B22 * Y1*Y1 + B11* Y1 )
    TH12 = B00 + B11*Y12 + B22* Y12 **2
    TH22 = B00 + B11*Y22 + B22* Y22 **2
    T1 = (TH1 * 3.14159)/180.
    T12 = (TH12 * 3.14159)/180.
    T2 = (TH2 * 3.14159)/180.
    T22 = (TH22 * 3.14159)/180.
    T3 = (TH3 * 3.14159)/180.
    HZ1 = HR1 * SIN ( T1 )
    HZ12 = HR12* SIN ( T12)
    HZ2 = HR2 * SIN ( T2 )
    HZ22 = HR22* SIN ( T22)
    HZ3 = HR3 * SIN ( T3 )
    A1 = H/6.* (HZ1 + 4.*HZ12 + HZ2)
    A2 = H/6.* (HZ2 + 4.*HZ22 + HZ3)
    IF(Y1)21,21,22
  22 HZA1 = A/Y1
    GO TO 32
  21 HZA1 = 0.
  32 A = A + A1
    HZA2 = A/Y2
    A = A + A2
    BZA1 = HZA1 * 4.* 3.14159E-7

```



```

BZA2 = HZA2 * 4.* 3.14159E-7
SA1 = 3.14159 *Y1*Y1
SA2 = 3.14159 *Y2*Y2
FLUX1 = SA1* BZA1
FLUX2 = SA2* BZA2
AT = DELTA * .5456
DIA1 = Y12 * 2.* 3.14159
DIA2 = Y22 * 2.* 3.14159
R1 = (RHO * DIA1)/AT
R2 = (RHO * DIA2)/AT
E1 = FLUX1 * 4.* 3300.
E2 = FLUX2 * 4.* 3300.
C1 = E1/R1
C2 = E2/R2
FORCE1 = 4.* 3.14159E-7 * HR12 * DIA1 * C1
FORCE2 = 4.* 3.14159E-7 * HR22 * DIA2 * C2
PRESS1 = FORCE1/(DIA1 * H)
PRESS2 = FORCE2/(DIA2 * H)
PHI1 = -(TH12 + 90.)
PHI2 = -(TH22 + 90.)
WRITE (3,20) Y12, FORCE1, PRESS1, PHI1
WRITE (3,20) Y22, FORCE2, PRESS2,PHI2
20 FORMAT ( F15.5, 2E20.5, F15.4)
IF (Y3 - 7.0678 ) 2,1,1
99 STOP
END

```

REFERENCES

1. Wier, D. D., B. J. Ball, C. G. Catledge, and L. J. Hill, Development of a Valid Mathematical Formula or Group of Formulas to Establish Within an Accuracy of 5% the Inductance Audio Range Resulting in Beryllium Coil Assemblies Final Report, unpublished, Mississippi State University, 1966.
2. Gourishankar, Vembu, Electromechanical Energy Conversion, Scranton, 1965, pp. 204-205.
3. Ibid.
4. Skilling, Hugh H., Electric Transmission Lines, New York, 1951, pp. 136-137.
5. Fitzgerald, A. E. and Charles Kingsley, Jr., Electric Machinery, New York, 1961, pp. 8-9.
6. Skilling, pp. 136-137.
7. Ibid, p. 150.
8. Fitzgerald and Kingsley, pp. 8-9.
9. Wier, Ball, Catledge, and Hill, pp. 107-108.
10. Ramo, Simon and John R. Whinnery, Fields and Waves in Modern Radio, London, 1964, pp. 236-238.
11. Thomas, George B., Jr., Calculus and Analytic Geometry, London, 1961, p. 386.
12. Hayt, William H., Jr., Engineering Electromagnetics, New York, 1958, pp. 200-203.
13. Wier, Ball, Catledge, and Hill, pp. 107-108.
14. Gourishankar, pp. 204-205.
15. Hayt, p. 11.

BIBLIOGRAPHY

- Fitzgerald, A. E., and Charles Kingsley, Jr., Electric Machinery. New York, McGraw-Hill, 1961.
- Gourishankar, Vembu, Electromechanical Energy Conversion. Scranton, International, 1965.
- Hayt, William H., Jr., Engineering Electromagnetics. New York, McGraw-Hill, 1958.
- Hudson, Ralph G., The Engineer's Manual. New York: John Wiley and Sons, 1961.
- Kraus, J. D., Electromagnetics. New York, McGraw-Hill, 1953.
- Ramo, S., and John R. Whinnery. Fields and Waves in Modern Radio. 2nd ed., New York, John Wiley and Sons, 1964.
- Skilling, Hugh H., Electric Transmission Lines. New York, McGraw-Hill, 1951.
- Thomas, George B., Jr., Calculus and Analytic Geometry. 3rd ed. Reading, Addison-Wesley, 1961.
- Ward, Robert P., Introduction to Electrical Engineering. Englewood Cliffs, Prentice-Hall, 1960.
- Weast, Robert C., Samuel M. Selby, and Charles D. Hodgeman. Standard Mathematical Tables. 14th ed., Cleveland, Chemical Rubber, 1965.
- Wier, D. D., B. J. Ball, C. G. Catledge, and L. J. Hill. Development of a Valid Mathematical Formula or Group of Formulas to Establish Within an Accuracy of 5% the Inductance Audio Range Resulting in Beryllium Coil Assemblies. Mississippi State University, 1966.